

The Effect of Climate Change on Extreme Sea Levels along Victoria's Coast

A Project Undertaken for the Department of Sustainability
and Environment, Victoria as part of the 'Future Coasts'
Program

Kathleen L. McInnes, Ian Macadam and Julian O'Grady

November 2009

Enquiries should be addressed to:

Dr Kathleen L. McInnes
CSIRO Marine and Atmospheric Research
Private Bag 1
Aspendale Vic 3195

Distribution list

Chief of Division	1
Project Manager	1
Client	1
Kathleen McInnes	1
Ian Macadam	1
Julian O'Grady	1
National Library	1
CMAR Libraries	1

Copyright and Disclaimer

© 2009 CSIRO To the extent permitted by law, all rights are reserved and no part of this publication covered by copyright may be reproduced or copied in any form or by any means except with the written permission of CSIRO.

Important Disclaimer

CSIRO advises that the information contained in this publication comprises general statements based on scientific research. The reader is advised and needs to be aware that such information may be incomplete or unable to be used in any specific situation. No reliance or actions must therefore be made on that information without seeking prior expert professional, scientific and technical advice. To the extent permitted by law, CSIRO (including its employees and consultants) excludes all liability to any person for any consequences, including but not limited to all losses, damages, costs, expenses and any other compensation, arising directly or indirectly from using this publication (in part or in whole) and any information or material contained in it.

Contents

Foreword	4
Glossary	5
Executive Summary	9
1. Introduction	13
2. Methodology	15
2.1 Overview	15
2.2 Identification of Past Extreme Sea Level Events	16
2.3 Hydrodynamic Modelling of Storm Surge	17
2.4 Extreme Event Analysis	18
2.5 Tides	19
2.6 Evaluation of Storm Tide Return Periods	21
2.7 Development of Inundation Layers	22
3. Climate Change Scenarios for Sea Level and Wind Speed	25
3.1 Sea Level Rise.....	26
3.2 Wind Speed	27
4. Extreme Sea Level Analysis	29
4.1 Storm Surge Return Levels	29
4.2 Storm Tide Return Levels	31
5. Inundation and Exposure Analysis	36
5.1 Portland.....	36
5.2 Port Fairy	39
5.3 Barwon Heads	41
5.4 Tooradin.....	43
5.5 Seaspray and The Honeysuckles	45
6. Summary and Future Work	48
6.1 Summary and Discussion	48
6.2 Recommendations for Future Work	50
Acknowledgments	52
References	53

List of Figures

Figure 1 The possible contributions to extreme sea levels at the coast.	13
Figure 2 Schematic diagram illustrating modelling approach used in this study.	15
Figure 3 The horizontal domain of the 5 km resolution model grid with the red rectangle indicating the extent of the 1 km resolution Bass Strait storm surge model grid.	18
Figure 4: Comparison between frequency histograms derived using tide constituents from the various tide gauges along the Victorian coast with those estimated from hydrodynamic modelling of tides at the same location.	21
Figure 5: Digital Elevation Data in m (AHD) sourced from the Victorian Department of Sustainability and Environment’s ‘Future Coasts’ LiDAR survey for the coastlines of western Victoria (a) and eastern Victoria (b). The five rectangular regions show areas containing extensive low-lying terrain (less than 2 m AHD) which have been selected for inundation analysis.	23
Figure 6: The spatial pattern of 1 in 100 year storm surge heights for the Victorian coast under late 20 th Century climate conditions. Note that these do not include a tidal component. Values are in metres relative to late 20 th Century mean sea level. P=Portland, PF=Port Fairy, Wa=Warrnambool, AB=Apollo Bay, L=Lorne, SP=Stony Point, K=Kilcunda, VB=Venus Bay, Wk=Walkerville, PW=Port Welshpool, S=Seaspray, LE=Lakes Entrance, PH=Point Hicks.	29
Figure 7: The spatial pattern of 1 in 100 year storm tide heights for the Victorian coast under (a) late 20 th Century climate conditions, (b) including scenario 2 wind speed increases for 2100 without sea level rise , (c) for scenario 2 in 2100. Values are in metres relative to late 20 th Century mean sea level.	32
Figure 8: Storm tide height return period curves for selected Victorian locations under current climate conditions and climate change scenarios as indicated in Table 4. Note that * denotes scenarios that incorporate wind speed changes. Note that the curves for Port Welshpool have been obtained from McInnes et al. (2009), in which high resolution modelling of this location was undertaken.	35
Figure 9: Land vulnerable to inundation during a 1 in 100 year storm tide under current climate conditions and various scenarios of future sea level rise for (a) the Portland region (b) Portland Harbour and (c) Surry River.	38
Figure 10: Land vulnerable to inundation during a 1 in 100 year storm tide under current climate conditions and various scenarios of future sea level rise for (a) the coastline from Port Fairy to Warrnambool, (b) Port Fairy and (c) Warrnambool.	40
Figure 11: Land vulnerable to inundation during a 1 in 100 year storm tide under current climate conditions and various scenarios of future sea level rise for the Barwon Heads region.	42
Figure 12: Land vulnerable to inundation during a 1 in 100 year storm tide under current climate conditions and various scenarios of future sea level rise for the Tooradin region.	44
Figure 13: Land vulnerable to inundation during a 1 in 100 year storm tide under current climate conditions and various scenarios of future sea level rise for Seaspray and The Honeyuckles.	46

List of Tables

Table 1: Composition of complete time series of daily maximum sea level residuals used for storm surge identification*.....	17
Table 2: Tidal characteristics at tide gauges in Bass Strait. Heights, in metres relative to mean sea level, are given for Highest Astronomical Tide (HAT), the Mean High Water Springs (MHWS) and the Mean High Water Neaps Higher (MHWN). Note that at stations marked by an asterisk, the tides are predominantly diurnal, and so the average value of the high tides is given by the Mean Higher High Water (MHHW) and Mean Lower High Water (MLHW) (see the Australian Tide Tables for more information).....	19
Table 3: The phase and amplitude errors of four tide constituents evaluated from a hydrodynamic model simulation of tides at four locations along the Victorian coast.	20
Table 4: Climate change scenarios considered in the present study. Scenario 1 considers the IPCC (2007) high scenario for mean sea level, scenario 2 combines the high sea level rise scenario with the equivalent high annual averaged wind speed change averaged over Bass Strait from CSIRO and Australian Bureau of Meteorology (2007). Scenario 3 considers the upper sea level rise scenario developed for the Netherlands Delta Committee and scenario 4 considers the upper sea level scenario proposed by Rahmstorf (2007). Note that asterisked values were not investigated in the present study.	27
Table 5: Storm surge height return levels for selected Victorian locations (see Figure 6) under current climate conditions and climate change scenarios as indicated in Table 4. All values are in metres relative to late 20 th Century mean sea level. Values for Port Welshpool and Lakes Entrance are from McInnes et al. (2009), in which high resolution modelling was undertaken. Higher resolution studies of sections of the coastline using different methodologies may yield different return levels than this study of the entire Victorian coast.	30
Table 6: Storm tide height return levels for selected Victorian locations (see Figure 6) under current climate conditions and climate change scenarios as indicated in Table 4. All values are in metres relative to late 20 th Century mean sea level. Values for Port Welshpool and Lakes Entrance are from McInnes et al. (2009), in which high resolution modelling was undertaken. Higher resolution studies of sections of the coastline using different methodologies may yield different return levels than this study of the entire Victorian coast.	33
Table 7: Summary of the exposure of land parcels and roadways in the Portland region to inundation under current climate conditions and various climate change scenarios.	37
Table 8: Summary of the exposure of land parcels and roadways in the Port Fairy region to inundation under current climate conditions and various climate change scenarios.	41
Table 9: Summary of the exposure of land parcels and roadways in the Barwon Heads region to inundation under current climate conditions and various climate change scenarios.	43
Table 10: Summary of the exposure of land parcels and roadways in the Tooradin region to inundation under current climate conditions and various climate change scenarios.	45
Table 11: Summary of the exposure of land parcels and roadways in the Seaspray region to inundation under current climate conditions and various climate change scenarios.	47

FOREWORD

This report has been prepared as part of the Future Coasts Program. The Future Coasts Program is a joint program of the Victorian Departments of Sustainability and Environment and Planning and Community Development.

The report provides data and information about the potential extent of coastal inundation due to extreme sea levels under a range of sea level rise scenarios.

The sea level rise scenarios used were selected by the Future Coasts Program to align with the Victorian Coastal Strategy 2008 (VCS) policy of planning for not less than 0.8 m sea level rise by 2100. As scientific data become available the VCS policy of planning for sea level rise of not less than 0.8 m by 2100 will be refined and may be superseded by national benchmarks. The minimum scenario considered in this study aligns with the VCS by using the international Intergovernmental Panel on Climate Change A1FI scenario of sea level rise.

This study has been undertaken on a state-wide scale, as part of a state-wide coastal vulnerability assessment. In order to provide spatially complete data on extreme sea levels, the study has employed computer modelling of storm surges and tides. The outputs are therefore bound by limitations in computing capacity and input datasets used by the computer model. It is possible that higher resolution studies of sections of the coast, and studies that use a different methodology, will produce estimates of extreme sea levels that differ from those presented in this state-wide study.

This state-wide study provides a baseline of data for coastal decisions in the absence of other studies. In the instance where more localised vulnerability studies have been undertaken, it may be appropriate to draw on the data from those studies for coastal management and planning applications.

Our climate will change over the coming decades. This report will assist coastal planners and decision makers to make more informed decisions in preparing for change.

Future Coasts Program

Victorian Government, Department of Sustainability and Environment

GLOSSARY

1 in 100 year storm tide	The storm tide level that is expected to be exceeded <i>on average</i> only once every 100 years. It is important to note that this is a statistical average, and exceedance events may actually occur more frequently within a specified period.
AHD	Australian Height Datum. The reference datum for heights in Australia. It attempts to measure heights above the geoid that closely coincide with mean sea level over the ocean. It was calculated around Australia in 1971 based on accurate levelling adjusted to zero at Mean Sea Level (MSL) at 30 tide gauges around mainland Australia. AHD is therefore approximately equal to mean sea level at most locations.
ARI	Average Recurrence Interval. The <i>average</i> time interval between two events that exceed a specified level. For example, the <i>average</i> time interval between two 1 in 100 year storm tides is 100 years. It is implicit in this definition that the intervals between events are generally random and will not all be equal to the ARI.
Confidence interval	A statistical range with a specified probability that a given parameter lies within the range.
DEM	Digital Elevation Model. A data set in electronic form that describes the topography of the land surface.
Diurnal tides	Tides occurring once per day, i.e. one high tide and one low tide per 24 hour period.
Ebb tides	The seaward flow in estuaries or tidal rivers during a tidal phase of lowering water level (opposite is 'flood tide').
Extreme event analysis	See extreme value statistical analysis.
Extreme value statistical analysis	A widely-used statistical methodology for drawing inferences about the extremes of a random process using only data on relatively extreme values of that process (Coles, 2001).
Frequency distribution	Number of times a given quantity (or group of quantities) occurs in a set of data. For example, the frequency distribution of tide heights shows how often tides are at a particular height. It is plotted either as a step-column chart (histogram) or as a line-chart (histograph).
Frequency histogram	A step-column chart indicating how frequently the particular value or quantity occurs (see frequency distribution).
Frictional attenuation	The slowing of currents due to the effect of friction exerted by the sea floor. A shallow column of water will be more effectively slowed than a deeper column of water.
HAT	Highest Astronomical Tide. The highest level that can be predicted to occur under average meteorological conditions and under any combination of astronomical conditions. This level will not be reached every year (Australian Tide Tables, 2007). HAT is not the most extreme sea level that can be reached as storm surges can add an additional component to sea level.
Hydrodynamic model	A computer model that solves mathematical equations that govern the

	vertical rise and fall of the ocean surface and the speed and direction of water movements. The mathematical equations are usually solved at discrete locations across a spatial region.
Inundation exposure analysis	Analysis of land areas that are vulnerable to inundation from particular levels of storm tide and mean sea level rise.
Joint probability	A statistical measure representing the likelihood of two events occurring together and at the same point in time. Joint probability is the probability of event Y occurring at the same time event X occurs.
JPM	Joint Probability Method (see joint probability).
Mean sea level	The height of the sea surface averaged over a period of time such that changes in sea levels due to waves and tides are averaged out.
MHHW	Mean Higher High Waters. For locations that experience a semi-diurnal tide regime (i.e. two high tides and two low tides per day), the MHHW is the mean (over a long period of time) of the higher of the two daily high tides.
MHWN	Mean High Water Neaps. The height of mean high water neaps is the average throughout the year of two successive high waters during those periods of 24 hours when the range of the tide is at its least.
MHWS	Mean High Water Springs. The height of mean high water springs is the average throughout the year of two successive high waters during those periods of 24 hours when the range of the tide is at its greatest.
MLHW	Mean Lower High Waters. For locations that experience a semi-diurnal tide regime (i.e. two high tides and two low tides per day), the MLHW is the mean (over a long period of time) of the lower of the two daily high tides.
MSLP	Mean Sea Level Pressure. The pressure of the atmosphere at mean sea level.
Neap tides	Term given to the tide that occurs two weeks after a new moon or full moon: at these times the tidal range is smaller i.e. high tides are not as high and the low tides are not as low as the corresponding tides during spring tides. This is because the alignment of the Sun, Earth and the moon form a right angle so the net gravitational effect of the moon and Sun on the Earth is weaker.
Probability distributions	A description of the possible values of a random variable, and of the probabilities these values will occur.
Projection	A data set describing the future that incorporates information on uncertainty.
Return period	A return period, also known as an Average Recurrence Interval, is an estimate of the average interval of time between two events that exceed a particular magnitude.
Root mean square (rms) error	The rms error is a statistical measure of the difference between two sets of values that can be compared in a pairwise fashion. The rms difference between two time-varying series is the square root of the mean average of the sum of the squares of the differences between each corresponding pair of values.

Satellite altimeter	A satellite mounted instrument that measures the time taken by a radar pulse to travel from the satellite antenna to the surface and back to the satellite receiver. Combined with precise satellite location data, altimetry measurements can be used to derive sea-surface heights.
Scenario	An internally consistent description of the evolution of a system. Scenarios are often used as a tool for risk management. In the context of future climate conditions, a set of scenarios is often adopted to represent the uncertainty in the future evolution of relevant but highly uncertain variables (e.g. global carbon dioxide emissions).
Semi-diurnal tides	Tides occurring twice per day; i.e. two high tides and two low tides in a 24 hour period.
Spring tides	Term given to the tide that occurs at the time of a new moon or full moon: at these times the high tides are higher and the low tides are lower than the corresponding tides during neap tide because the gravitational effects of the straight-line alignment of the moon, Earth, and Sun are stronger.
SRES	Special Report on Emission Scenarios was a report prepared by the Intergovernmental Panel on Climate Change (IPCC) for the Third Assessment Report (TAR) in 2001. SRES provides future emission scenarios to be used for driving global circulation models to develop climate change scenarios.
Storm surge	Elevated sea levels caused by the effect of falling mean sea level pressure and strong winds during severe weather events.
Storm tide	The combination of storm surge with astronomical tide.
Storm tide surface	A two dimensional surface representing the height of a storm tide across an area of the sea.
Tidal amplitude	The magnitude of the difference in elevation between low and high tides at a particular point in a body of water.
Tidal constants	Another term for tidal constituents.
Tidal constituents	The components of the tide, each described by a particular amplitude and phase, which contribute to the total tidal signal. The main tidal constituent is the lunar semi-diurnal (half daily) or M2 tide which has a period of 12.42 hours. Other lunar semidiurnal constituents are the N2, S2 and K2 with periods of 12.60, 12.00 and 11.97 hours respectively. The diurnal (daily) constituents, O1, P1 and K1 have periods of 25.82, 24.07 and 23.93 hours respectively. Each of these constituents contributes amplitudes of at least 0.05 m in Bass Strait. Contributions to tides also occur on fortnightly, monthly, semi-annual and annual time scales. The total height of the tide can be calculated by summing the contributions from the various constituents (harmonic superposition).
Tide gauge	An instrument to measure the local sea level relative to a nearby geodetic benchmark. The most commonly used tide gauge measurement system consists of a float operating in a stilling well. Surveys of the tide gauge site are performed regularly to account for any settling of the site.

Tidal period	The amount of time between two successive high tides. The period of the constituent relates to the phase in that it represents the time required for the phase to change through 360°.
Tidal phase	An angular measure of the time of the maximum value of a periodic function, the entire period of the function being 360°.
Tide prediction	A term often used to describe the prediction of future tides based on summing together the time-varying sinusoidal components of the tide developed from the various tidal constituents (this is also referred to as harmonic superposition).
Tide simulation	A term usually used to describe the simulation of tide heights using a hydrodynamic model (as opposed to tide prediction). Both approaches can be used to predict future tides. However, the tide prediction approach while computationally efficient, requires prior knowledge of the tidal constituents at the location of interest and in practice, this is usually only where tide gauges are located or have been located. On the other hand, a hydrodynamic model can be used to determine how the tides behave across the entire model domain. Using a hydrodynamic model for this purpose requires that the tides can be predicted on the model's lateral boundaries, but since these boundaries are generally located well offshore, gridded tide constituent data from global tide models are available for this purpose and are reasonably accurate in the deep ocean. Such data are less reliable in shallow shelf seas due to the spatial resolution of the global tide models.

EXECUTIVE SUMMARY

The study documented in this report has been undertaken as part of the Victorian Government's Future Coasts Program. The first part of the study estimates extreme sea levels along Victoria's coastline under current climate conditions. The impact of climate change on future extreme sea levels is then explored. Finally, for five low-lying regions along the coast, a Digital Elevation Model (DEM) acquired as part of the Future Coasts Program is used to assess potential vulnerability to inundation due to extreme sea levels under current and future climate conditions.

Extreme sea levels along the Victorian coast usually occur as a result of the combination of tides with storm surges associated with weather systems that bring westerly winds to the south coast of Australia. In this study, extreme sea levels are estimated using an approach similar to that of McInnes et al (2009a), whereby tide and surge heights are evaluated separately and then combined to estimate 'storm tide' heights. A hydrodynamic model is used to estimate tide and surge heights for the entire Victorian coast and return periods are estimated using extreme value statistical analysis.

Climate change is expected to influence the height and frequency of extreme sea level events along the Victorian coast through increases in mean sea level and changes in wind speed in Bass Strait. As with other aspects of climate change, projections of future mean sea level rise and changes in wind speed are inherently uncertain. Hence extreme sea levels are evaluated for several different plausible climate change scenarios (see Table E1). Two scenarios incorporate estimates of sea level rise by Hunter (2009) that correspond to high-end estimates of sea level rise over the 21st Century from the Fourth Assessment Report of the Intergovernmental Panel on Climate Change (IPCC, 2007). These estimates are consistent with the Victorian Coastal Strategy (2008) and the IPCC's SRES A1FI scenario for future greenhouse and aerosol emissions (Nakićenović and Swart, 2000), which matches recent observations of global carbon dioxide emissions (Raupach et al. 2007). The high-end A1FI sea level rise estimates are considered both with and without consistent high-end estimates of wind speed increases in Bass Strait obtained from recent climate change projections developed for Australia (CSIRO and Australian Bureau of Meteorology, 2007).

The observed rate of global sea-level rise since 1990 corresponds to the upper bound of estimates from the IPCC's Third Assessment Report (IPCC, 2001) projections (Rahmstorf et al., 2007), causing concern that values of sea level rise derived from global climate model simulations may be underestimating one or more of the model contributions to sea level rise. Hence two climate change scenarios incorporating sea level rise estimates higher than those of the IPCC (2007) were also investigated.

Table E2 presents 1 in 100 year storm tide levels at selected locations along the Victorian coast for current climate conditions and for each of the future climate change scenarios summarised in Table E1. This study finds that 1 in 100 year storm tide levels along the coast are highest in and around Western Port Bay, where they exceed 2.0 m under current climate conditions. Storm tide return levels are also high along the open coastline from just west of Port Phillip Heads to Wilsons Promontory, exceeding 1.8 m under current climate conditions. It should be noted that the methodology developed in this study, as well as the bathymetric and atmospheric

data sets and resolution of the hydrodynamic models, have been guided by the desire to provide data for the entire Victorian coast within the limitations of the available computing and data resources. It is possible that higher resolution studies of sections of the coastline utilising different methodologies and data sets may yield different return levels.

Table E1: Climate change scenarios considered in the present study. Scenario 1 considers the IPCC (2007) high scenario for mean sea level, scenario 2 combines the high sea level rise scenario with the equivalent high annual averaged wind speed change averaged over Bass Strait from CSIRO and Australian Bureau of Meteorology (2007). Scenario 3 considers the upper sea level rise scenario developed for the Netherlands Delta Committee and scenario 4 considers the upper sea level scenario proposed by Rahmstorf (2007). Note that asterisked values were not investigated in the present study.

Future climate scenario			2030	2070	2100
1	IPCC 2007 A1FI scenario Hunter (2009)	Sea level rise (m)	0.15	0.47	0.82
2	IPCC 2007 A1FI scenario in combination with 'high' wind speed scenario	Sea level rise (m)	0.15	0.47	0.82
		Wind speed increase (%)	4	13	19
3	Netherlands Delta Committee Vellinga (2008)	Sea level rise (m)	0.20*	0.70*	1.10
4	Rahmstorf (2007) upper estimate	Sea level rise (m)	0.23*	0.74*	1.40

Table E2: 1 in 100 year storm tide height return levels for selected locations along the Victorian coast under current climate conditions and climate change scenarios as indicated in Table E1. All values are in metres relative to late 20th Century mean sea level. Higher resolution studies of sections of the coastline using different methodologies may yield different return levels than this study of the entire Victorian coast.

Location	Current Climate	2030			2070			2100			
		1	2	3	1	2	3	1	2	3	4
Portland	1.01	1.16	1.22	1.21	1.48	1.61	1.71	1.83	2.05	2.11	2.41
Port Fairy	1.05	1.20	1.25	1.25	1.52	1.67	1.75	1.87	2.09	2.15	2.45
Warrnambool	1.06	1.21	1.27	1.26	1.53	1.69	1.76	1.88	2.13	2.16	2.46
Apollo Bay	1.42	1.57	1.63	1.62	1.89	2.04	2.12	2.24	2.46	2.52	2.82
Lorne	1.69	1.84	1.91	1.89	2.16	2.33	2.39	2.51	2.74	2.79	3.09
Stony Point	2.08	2.23	2.30	2.28	2.55	2.73	2.78	2.90	3.14	3.18	3.48
Kilcunda	1.94	2.09	2.18	2.14	2.41	2.61	2.64	2.76	3.03	3.04	3.34
Venus Bay	1.96	2.11	2.20	2.16	2.43	2.64	2.66	2.78	3.06	3.06	3.36
Walkerville	1.98	2.13	2.22	2.18	2.45	2.65	2.68	2.80	3.08	3.08	3.38
Port Welshpool	1.63	1.78	1.84	1.83	2.10	2.27	2.33	2.45	2.68	2.73	3.03
Seaspray	1.50	1.65	1.73	1.70	1.97	2.18	2.20	2.32	2.64	2.60	2.90
Lakes Entrance	1.04	1.19	1.24	1.24	1.51	1.66	1.74	1.86	2.09	2.14	2.44
Point Hicks	1.36	1.51	1.59	1.56	1.83	2.01	2.06	2.18	2.45	2.46	2.76

For the high-end A1FI sea level rise estimates considered, the contribution of consistent high-end estimates of wind speed increase to increases in extreme storm surge heights is considerably smaller, by a factor of more than two, than the contribution of sea level rise. It therefore seems likely that climate change will have a greater impact on extreme storm surge heights through sea level rise than through wind speed changes. It follows that sea levels currently attained only during severe storms will be reached during much less extreme conditions in the future.

A simple inundation model was used to investigate the coastal terrain that would be vulnerable to inundation under 1 in 100 year storm tide conditions under both current and future climate conditions. Five regions along the Victorian coast were selected for inundation analysis on the basis that they contained extensive areas of terrain below 2 m elevation: Portland, Port Fairy, Barwon Heads, Tooradin and Seaspray

Under current climate conditions, the areas most vulnerable to inundation from a 1 in 100 year storm tide are generally beach front and low-lying wetland and coastal reserve areas, as summarised below:

- Portland region: Minimal inundation.
- Port Fairy region: The banks of the Moyne River and Belfast Lough at Port Fairy and the lower reaches of the Merri River at Warnambool.
- Barwon Heads region: The lower reaches of the Barwon River and low-lying land behind the dune system at Breamlea.
- Tooradin region: An extensive area of coastal land extending inland of the South Gippsland Highway between Cardinia Creek and Sawtells Inlet and inland areas to the north of Warneet.
- Seaspray region: Lakes Reeve and Denison and the banks of the Merriman Creek.

Under future climate conditions, changes in the areas most vulnerable to inundation from a 1 in 100 year storm tide can be summarised as follows:

- Portland region: Minimal additional inundation until after 2070. By 2100, foreshore regions around Portland Harbour and Nuns Beach and the lower reaches of the Surry River, including low-lying terrain extending to the east and west of the river.
- Port Fairy region: Minimal additional inundation until after 2030. By 2070, extensive additional area adjacent to Belfast Lough at Port Fairy and the Merri River at Warnambool. By 2100, additional area at the northeast of Belfast Lough, in Port Fairy township and Kelly Swamp, and if the higher estimates of sea level rise eventuate (scenarios 3 and 4 of Table E1) Lake Pertobe, at Warnambool.
- Barwon Heads region: By 2030, a small additional area along the Barwon River near Geelong and along Thomson Creek. By 2070, parts of Ocean Grove adjacent the Barwon River and low-lying land east of Breamlea. By 2100, if the higher estimates of sea level rise eventuate (scenarios 3 and 4 of Table E1), extensive inundation of the township of Barwon Heads and the region to the west of the township.

- Tooradin region: Incrementally more extensive areas north of the South Gippsland Highway as the 21st Century progresses. By 2100, significant additional areas west of Tooradin.
- Seaspray region: By 2030 and 2070, incrementally larger parts of the township of Seaspray. By 2100, complete inundation of the township of Seaspray and, if the higher estimates of sea level rise eventuate (scenarios 3 and 4 of Table E1), extensive inundation of The Honeysuckles.

In using the results of this study, it is important to be aware of caveats associated with the methodology used. Estimating the contribution of waves to extreme sea levels, which is generally much smaller than that of a storm surge, was beyond the scope of the study and future work should aim to quantify this contribution along the Victorian coastline. The inundation analysis presented was performed using a simple technique that does not take into account some of the physical factors that will influence the degree of inundation that will occur and their omission may have led to an overestimation of the degree of inundation. Future work may seek to quantify this overestimation by explicitly modelling the temporal evolution of inundation during a storm tide event. Inundation due to storm tides is often accompanied by inundation due to rainfall. This additional contribution to inundation is not taken into account in this study and there would be benefit to investigating the potential for coincident storm tide and heavy rainfall events in the Victorian region under current and future climate conditions. Finally, this study has regarded the topography of the coastline as being constant throughout the 21st Century. However, during this time period, environmental processes, such as the erosion of beaches and soft cliffs, and the adaptive responses of society, such as renourishment of beaches to retain the existing coastline and the building of sea walls, have the potential to change the morphology of the shoreline. The consideration of these processes should be a priority area for future work.

Despite various limitations, the analysis presented in this study illustrates how different climate change scenarios may affect the degree of inundation that could potentially occur due to extreme sea levels in the future. The study identifies areas that will be most vulnerable to coastal inundation in the future and highlights thresholds of sea level rise that are important in the context of vulnerability and adaptation.

1. INTRODUCTION

Victoria's coastline is highly valued for its aesthetic, ecological, recreational and economic assets. Since the late 1990's, a rapid increase in the rate of internal migration from large cities to the coast, referred to as the Sea Change Phenomenon (Gurren et al., 2005), has led to an increase in development pressure in coastal towns and elsewhere along the coast. The increase in population pressure and the value of assets along the coast poses challenges for those responsible for the sustainable management of the coast. Climate change is creating a significant additional challenge to coastal management and will continue to do so for the foreseeable future. Rising sea levels and other changes to the climate system mean that the coast cannot be considered a static entity for the purposes of planning and management and the consequences of future climate change must be considered.

A range of natural hazards pose risks to Victoria's coastal regions. Low-lying coastal terrain is vulnerable to inundation during high sea level events caused by storm surges or due to increased riverine flows due to heavy rainfall. Soft shorelines may experience severe erosion during storm surge or high wave events. Such events may occur in isolation or in combination. Rising mean sea levels and possible changes in the behaviour of severe weather conditions are likely to increase the frequency and severity of extreme sea level events in the future.

Extreme sea level events are caused by severe storms. Figure 1 illustrates the various possible contributions to extreme sea levels. Storm surges are the temporary increases in coastal sea levels caused by the falling atmospheric pressure and severe winds during storms. Often accompanying the storm surge is an additional increase in water level due to the cumulative effect of breaking waves on the open coast, which produces wave setup. The magnitude of the wave setup is related to the height of the offshore waves and is usually much smaller than the storm surge. Wave runup, is the maximum inland penetration of water that is caused by the breaking of individual waves at the coast. The present study is concerned with evaluating the storm surge and tidal contributions to extreme sea levels and does not include an assessment of wave runup and wave setup. The combination of the storm surge and the astronomical tide is defined here as a storm tide.

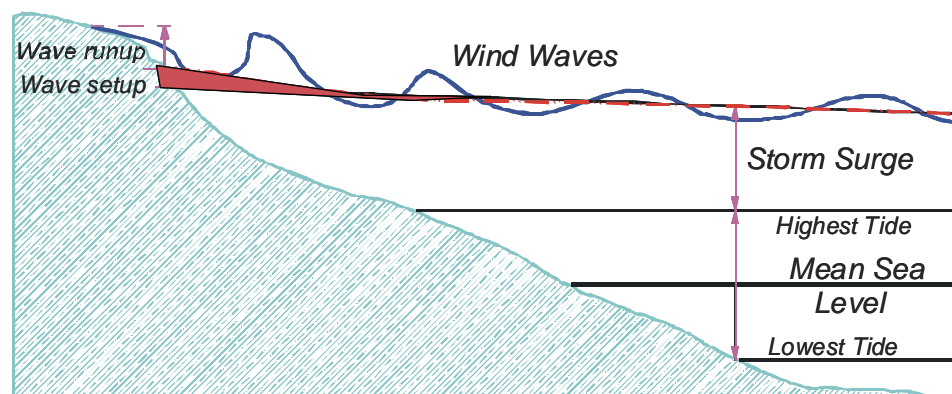


Figure 1 The possible contributions to extreme sea levels at the coast.

The study documented in this and a companion report; 'The Effect of Climate Change on Extreme Sea Levels in Port Phillip Bay' have been undertaken as part of the Victorian Government's 'Future Coasts' Program. It employs computer models and statistical techniques to develop information on the extreme sea level hazard along Victoria's coast. It also explores the impact of a range of plausible climate change scenarios on sea level extremes under future climate conditions. A Digital Elevation Model (DEM) of Victoria's coast, acquired as part of the Future Coasts Program, is used in combination with the extreme sea levels and climate scenarios to evaluate potential inundation at a selection of sites along Victoria's coast.

The remainder of this report is structured as follows. Section 2 briefly describes the method. Section 3 presents and discusses the future climate change scenarios used in this study. Section 4 describes the extreme sea level results. Section 5 investigates the potential inundation at several selected sites. Finally a discussion of the results and conclusions are presented in section 6.

2. METHODOLOGY

2.1 Overview

For the purposes of planning and engineering design, extreme sea level events are commonly expressed in terms of return periods. A return period is defined as the average amount of time between events that exceed a particular level. Therefore a 1 in 100 year sea level is the sea level that is exceeded on average once every 100 years. In this study, a simple inundation model is used in combination with the Future Coasts DEM and maps of 1 in 100 year sea levels to identify parts of the Victorian coast that are vulnerable to inundation. The maps of 1 in 100 year sea levels are developed using both hydrodynamic and extreme value statistical modelling techniques.

The most important components of extreme sea levels along the Victorian coast are tides and storm surges; sea level elevations caused by the high winds and low mean sea level pressure associated with storms. In this study, these components are evaluated separately and then combined to estimate ‘storm tide’ heights using the well established Joint Probability Method (JPM) based on the work of Pugh and Vassie (1980) and Tawn and Vassie (1989). The approach used in this study is illustrated schematically in Figure 2 and the methodology for the analysis of surge and tide heights is described in the subsequent sections.

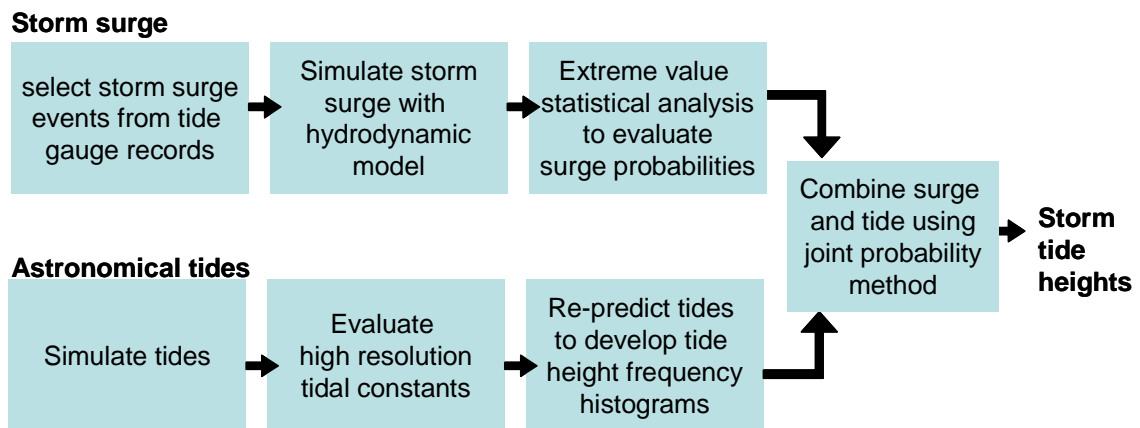


Figure 2 Schematic diagram illustrating modelling approach used in this study.

Previous studies have established that the main synoptic weather systems responsible for storm surges along the coastline of Victoria are west-to-east travelling cold fronts, which occur year round but tend to be more frequent and intense in the winter months (McInnes and Hubbert, 2003; McInnes et al., 2005a). The large spatial scale of these systems means that they impact a large stretch of coastline when they occur and so the resultant elevated coastal sea levels are well captured by the available tide gauge network. This is exploited by this study, which uses a selection of tide gauge records to identify a population of significant storm surge events occurring during the 1966-2003 period, for which largely complete tide gauge records were

available. Probabilities of extreme storm surge heights, which are required as input to the Joint Probability Method, are developed from an analysis of this population using the approach of McInnes et al. (2009a).

Although tide gauge records are used to identify the population of storm surge events on which the analysis is based, and could form the basis of an analysis of extreme sea levels at the locations where gauges are present, they are not sufficient to provide the spatially complete information needed to develop maps of 1 in 100 year sea levels. For this reason, a hydrodynamic model was used to simulate each of the storm surge events in the population.

Since the set of events were obtained from only a 38-year period, it was not possible to directly estimate probabilities for rare extreme storm surge heights from the model output. A theoretical statistical distribution for extreme values, the 2-largest Generalised Extreme Value (GEV) distribution (see Coles, 2001), was therefore fitted to the data at each model gridbox and used to extrapolate probabilities for extreme storm surge heights.

The procedure used for storm surge evaluation can be summarised as follows:

1. *Storm surge identification*: significant storm surge events are identified from tide gauge records
2. *Hydrodynamic modelling of surges*: each event is simulated with a hydrodynamic model and the maximum modelled surge peaks from each event is stored
3. *Extreme value analysis*: extreme value statistics are used to evaluate storm surge height probabilities

A procedure was also developed for evaluating tide height probability distributions that was required for subsequent use in the JPM. This procedure is summarised as follows:

1. *Tide simulation*: continuous hydrodynamic model simulation over several months to provide tide heights
2. *Tide height analysis*: analyse simulated tide heights to evaluate tidal constituents
3. *Tide height prediction*: the tide constituent data are used by a tide prediction model to recalculate tides over a full tidal cycle (18.6 years) and the heights are binned into classes to develop a tide height frequency distribution

2.2 Identification of Past Extreme Sea Level Events

The sea levels from 13 tide gauges along the northern Bass Strait coast were filtered to remove astronomical tides using the method of Godin (1972) to obtain the residual sea levels due to meteorological forcing¹. Three tide gauge records, for Portland, Point Lonsdale and Lakes Entrance were identified as key sources of data from which to identify extreme sea level residual events owing to their length, completeness and spatial coverage of the northern coastline of Bass Strait. Data gaps in these records were filled by developing linear regression relationships between these records and other available records and introducing data from the

¹ An alternative method to obtain sea level residuals, subtracting the predicted tide from the observed sea levels, has been found to be problematic during episodes of strong westerlies due to the stronger wind forcing influencing the phase of the tidal currents into and out of Bass Strait (McInnes and Hubbert, 2003, McInnes et al., 2009)

most correlated gauge for which data was available. Table 1 summarises the composition of the resulting complete sea level residual time series for Portland, Point Lonsdale and Lakes Entrance.

A population of extreme storm surge events was then identified from the three complete key time series of residuals. An event was defined as an episode during which sea level residuals exceeded a threshold, μ m, above a background level. Linear relationships between the Point Lonsdale time series minus its background time series and the other two key time series minus their background time series were established using linear regression. A μ value of 0.20 m was selected for Point Lonsdale and the linear relationships were used to estimate corresponding μ values for Portland and Lakes Entrance, 0.15 and 0.14 m respectively.

Table 1: Composition of complete time series of daily maximum sea level residuals used for storm surge identification*.

Key record	Alternative records used for filling data gaps in key record		
Portland 55%	Port MacDonnell 40% (0.91)	Geelong 3% (0.87)	Others 2% (0.82 to 0.97)
Point Lonsdale 96%	Queenscliff 2% (0.97)	Geelong 2% (0.93)	Others <1% (0.79 to 0.97)
Lakes Entrance 60%	Williamstown 32% (0.77)	West Channel Pile 8% (0.78)	Others <1% (0.62 to 0.74)

*Contributions to the complete time series are given as percentages of data points. Correlations between the key records and the alternative records are given in brackets.

Since a single meteorological event may elevate the sea levels at a number of tide gauges as it propagates through the region, the events identified at each of the three tide gauges were checked for overlapping dates and merged into a single set which encompassed the earliest start date (minus 24 hours to allow for model spin-up) and the latest completion date. A total of 489 events were identified from an effective 38 years of data, the duration of each event ranging from 2 to 11 days.

2.3 Hydrodynamic Modelling of Storm Surge

The model used in this study is a two-dimensional hydrodynamic model known as GCOM2D, which solves the depth-averaged hydrodynamic equations for currents and sea levels. Details of the model formulation can be found in Hubbert and McInnes (1999). Two model grids was set up so that the storm surges generated along the southeastern Australian coast could be adequately resolved with the computing resources available. Hourly currents and sea levels from simulations on an extensive 5 km resolution grid were applied as boundary conditions to simulations on a nested 1 km resolution grid (see Figure 3).

Topographic and bathymetric data for the 5 km grid were obtained from the AUSLIG 9 second DEM (Version 1) (http://www.ga.gov.au/nmd/products/digidat/dem_9s.htm) and the Geoscience Australia (formerly AGSO) 30 second bathymetry data set. On the 1 km grid the 3 arc-second (~90 m) Shuttle Radar Topography Mission data was used over land (<http://srtm.csi.cgiar.org/index.asp>).

The simulation of storm surges requires that the hydrodynamic model be forced with near-surface winds (typically winds at 10 m above the surface) and surface pressure. These meteorological variables were obtained from the U.S. National Center for Environmental Prediction (NCEP) reanalyses (Kalnay et al., 1996). Wind fields at 10 m above the surface were available on a $1.875^{\circ} \times 1.875^{\circ}$ global grid and the mean sea level pressure fields were available on a $2.5^{\circ} \times 2.5^{\circ}$ global grid every 6 hours from 1958 onwards. The NCEP data were interpolated spatially to the GCOM2D grid. At the conclusion of each simulation, the maximum sea level simulated by the model over the duration of the event was stored at each grid cell, yielding an array of peak storm surge heights for each event.

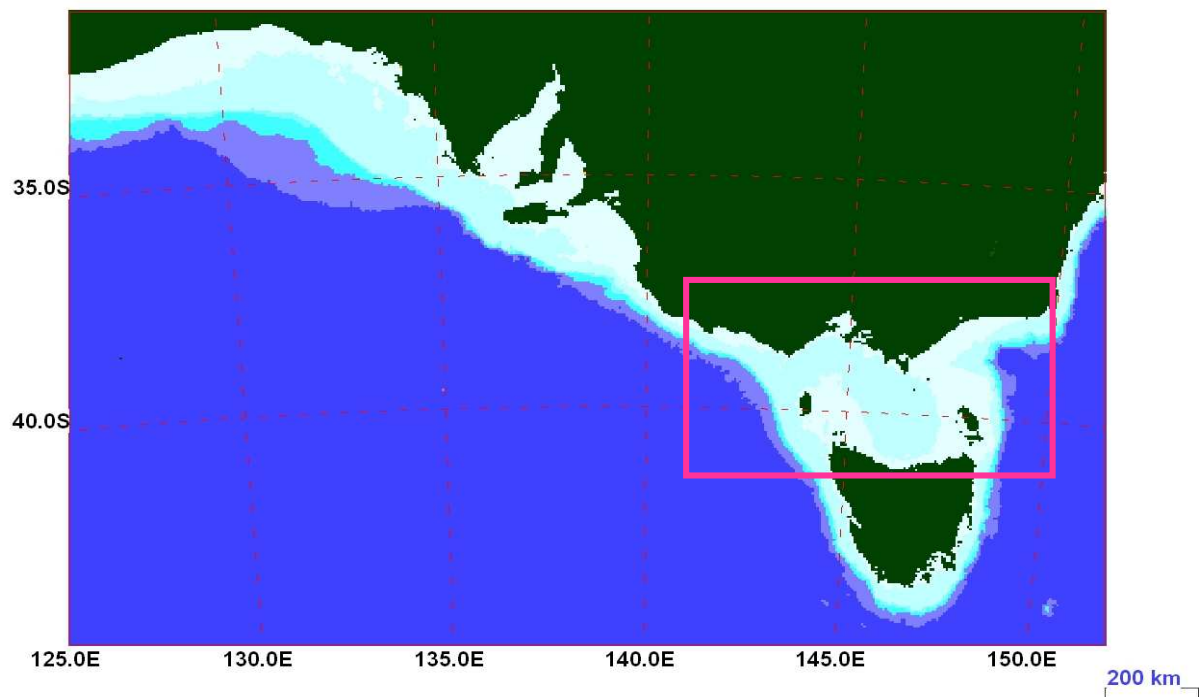


Figure 3 The horizontal domain of the 5 km resolution model grid with the red rectangle indicating the extent of the 1 km resolution Bass Strait storm surge model grid.

2.4 Extreme Event Analysis

For the purposes of planning and engineering design, storm surge or storm tide levels are commonly expressed in terms of return periods. A return period is defined as the average amount of time between events that exceed a particular level. Therefore a 1 in 100 year sea level is the sea level that is exceeded on average once every 100 years. It is important to note that this is a statistical average, and events exceeding the 1 in 100 year level may actually occur more frequently within the 100 year period. For data that span a shorter time interval than the return period value that is sought, the estimation of return levels relies upon a branch of statistical analysis that deals with extremes. Mathematical formulae which represent the behaviour of extreme events are fitted to the data and this provides a method to estimate return levels of extreme events over time intervals that are longer than those spanned by the data.

Since the population of events identified in the tide gauge records represented only a 38 year period, extreme value statistical methods were applied to evaluate return levels of extreme sea level events for longer time intervals. A number of alternative methods were investigated in McInnes et al., (2006) and the method selected was the r-largest Generalised Extreme Value (GEV) approach. In this approach the observed events are binned into yearly intervals and the GEV distribution is fitted to the set of events comprising the top r values from each year (see Coles, 2001). An r value of 2 was used in this study. From this analysis, probabilities of the occurrence of an event exceeding a particular level in a given year could be estimated.

2.5 Tides

The impact of a storm surge on coastal inundation is influenced by the height of the astronomical tides at the time of the surge. Tide heights vary on a range of time scales due to the relative movements of the Sun, Earth and moon. The tidal regime of Bass Strait is mixed with tides that exhibit mainly diurnal characteristics to the west of Apollo Bay and mainly semi-diurnal characteristics to the east. The height of the daily high and low tides also varies fortnightly from the higher spring tides that occur close to full and new moons to the lower neap tides which occur around a week either side of these times. Further variations occur on half-yearly and yearly cycles. A summary of the key characteristics of the tides at several tide gauges along the Victorian coast is given in Table 2. The highest tidal range occurs in the middle of Bass Strait. The tidal range at Lakes Entrance is lower owing to the strong attenuation of the tides inside the entrance to the Lakes.

Table 2: Tidal characteristics at tide gauges in Bass Strait. Heights, in metres relative to mean sea level, are given for Highest Astronomical Tide (HAT), the Mean High Water Springs (MHWS) and the Mean High Water Neaps Higher (MHWN). Note that at stations marked by an asterisk, the tides are predominantly diurnal, and so the average value of the high tides is given by the Mean Higher High Water (MHHW) and Mean Lower High Water (MLHW) (see the Australian Tide Tables for more information).

Name	Latitude	Longitude	HAT	MHWS MHHW *	MHWN MLHW *
Portland*	-38.35	141.62	0.69	0.44	0.18
Port Fairy*	-38.40	142.25	0.73	0.43	0.18
Apollo Bay*	-38.75	143.67	1.09	0.83	0.13
Lorne	-38.53	144.00	1.27	0.81	0.42
Stony Point	-38.37	145.22	1.56	1.11	0.67
Waratah Bay	-38.85	146.04	1.49	1.11	0.74
Port Welshpool	-38.70	146.45	1.30	0.95	0.57
Lakes Entrance*	-37.88	147.97	0.59	0.32	0.01
Point Hicks	-37.81	149.27	0.83	0.48	0.28

The periodic behaviour of the tides at a particular location can be described by a set of constant values referred to as tidal constituents. These describe the phase and amplitude of variations in the tide-producing forces. Knowledge of these constants allows tidal behaviour to be predicted and tide height frequency distributions suitable for input to the JPM to be generated. Tide

gauge data provide the information necessary to evaluate the tidal constituents and thus predict tides and develop tide height frequency distributions. However for the purposes of developing spatially complete maps of tide height, hydrodynamical modelling was used to generate tidal information on a grid comparable to that used for the storm surge modelling. The three-dimensional counterpart to GCOM2D (GCOM3D) was used for this purpose. GCOM3D (Hubbert 1993a, b) calculates water currents in both the horizontal and vertical planes. This is important for representing tides accurately as the vertical gradient of tidal currents affects the phase and amplitude of tides at the coast.

Model simulations with GCOM3D were carried out for several months using tidal heights from a global tidal model (Le Provost et al., 1995) as deep water boundary conditions. The time series of tide heights were then analysed in the same way as time series of tide gauge data to evaluate the amplitudes and phases of a set of tidal constituents.

In the running of GCOM3D, an iterative approach was adopted that involved running the model over several tidal cycles, calculating the root mean square errors of the modelled tidal signal at locations where tide gauge data existed and adjusting the boundary conditions until the rms errors were minimised. The final rms errors are a function of an amplitude error and a phase error. A sample of the errors at four tide gauges for the leading four diurnal and semi-diurnal constituents, M2, S2, O1 and K1 are given in Table 3.

Table 3: The phase and amplitude errors of four tide constituents evaluated from a hydrodynamic model simulation of tides at four locations along the Victorian coast.

location	latitude	longitude	error	M2	S2	O1	K1
Portland	-38.35	141.617	amplitude (m)	0.011	-0.009	-0.011	-0.031
			phase (deg)	7	6	2	9
Lorne	-38.5	143.983	amplitude (m)	-0.005	0.027	-0.015	-0.029
			phase (deg)	-8	-5	-3	1
Rabbit Island	-38.917	146.517	amplitude (m)	-0.017	-0.039	-0.008	-0.028
			phase (deg)	-14	-14	-1	3
Point Hicks	-37.8	149.267	amplitude (m)	0.027	-0.041	0.033	0.041
			phase (deg)	11	4	8	-2

The tide height frequency distributions required for the JPM were then developed for each grid cell of the storm surge model by running a tide prediction model (Foreman, 1977) using the derived tidal constituents and binning the resulting tide heights to develop a frequency histogram. A comparison of a frequency histogram developed using constituents derived from tide gauge data with those developed from the hydrodynamic modelling approach is presented in Figure 4 for Portland, Stony Point, Rabbit Island (at the entrance to Corner Inlet) and Point Hicks.

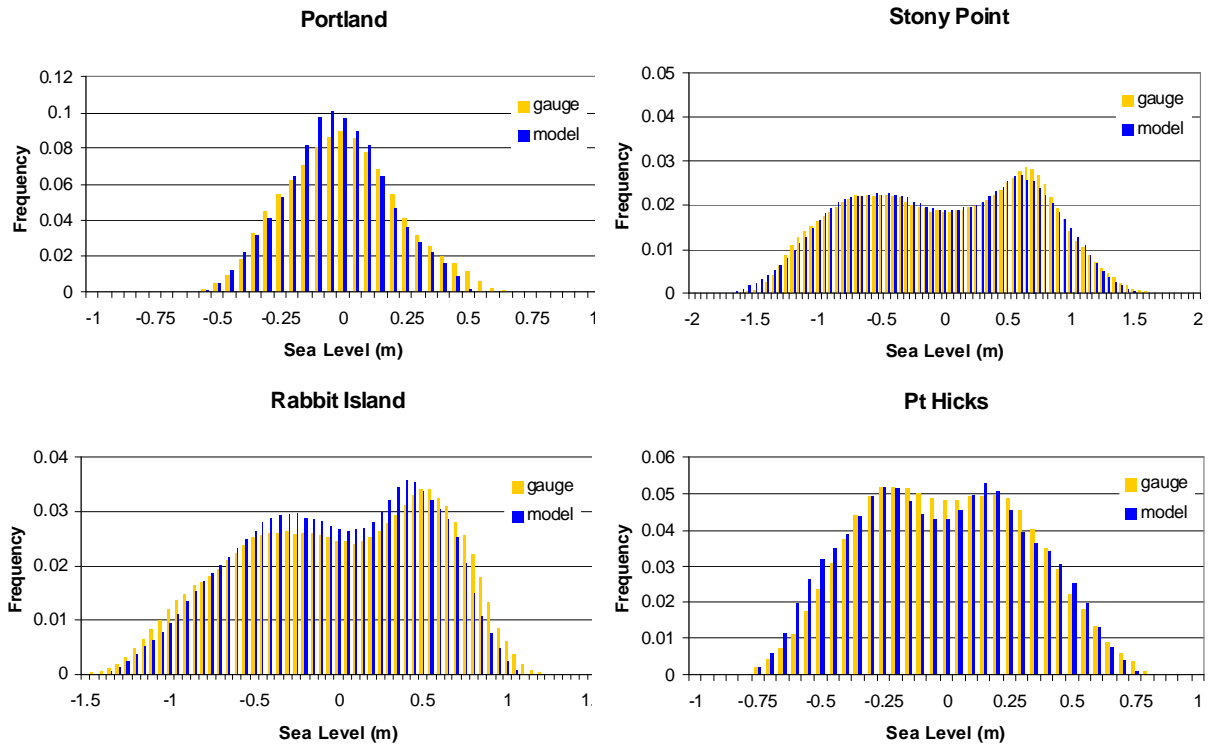


Figure 4: Comparison between frequency histograms derived using tide constituents from the various tide gauges along the Victorian coast with those estimated from hydrodynamic modelling of tides at the same location.

2.6 Evaluation of Storm Tide Return Periods

The common approach for combining the tidal distributions with those of storm surges is to assume independence between the tide and surge distributions. The approach, commonly referred to as the “joint probability” method (Pugh and Vassie, 1980), allows the combination of the two probability distributions for tide and surge height (see also Tawn and Vassie, 1989). The combination of the two probability distributions is achieved by randomly sampling a population of tide and surge values and summing them to develop a population of storm tide heights. Return periods for storm tide heights were estimated by ranking the sampled storm tides from largest to smallest and assigning the return period to the event height according to $R = N/r$ where R is the return level, N is the number of random samples and r is the rank of the event. To estimate the uncertainty in the storm tide estimates, 200 sets of 1000 storm tides were sampled and each set of 1000 storm tides was ranked from largest to smallest. From the 200 values associated with each rank (i.e. highest, second highest and so on), the mean was

taken to represent the best estimate storm tide height and the standard deviation was taken to represent the uncertainty in this associated with the random sampling.

In addition to the uncertainty in storm tide return levels due to the random sampling of tide and surge heights, three other significant types of uncertainty were accounted for. These were the uncertainty due to imperfections in the representations of tides by the hydrodynamic model, the uncertainty due to imperfections in the representations of storm surges by the hydrodynamic model and the uncertainty associated with the statistical fits to the extreme surge heights.

Standard errors were estimated for each uncertainty and combined by noting that, for N independent variables denoted by X_k for $k=1,N$, the combined error ΔX is derived using $\Delta X = \sqrt{\sum (\Delta X_k)^2, k=1,N}$. A selection of rms errors in the tidal constituents simulated by the hydrodynamic model are reported in Table 3 for several locations across Bass Strait and are incorporated directly into the formula (tide phase errors are not considered since their impact on the population of tides described by the developed tide height frequency histograms will be negligible). For the simulated storm surge heights, McInnes et al. (2009a) estimate that model biases for several locations across Bass Strait range from -0.036 to +0.035. We conservatively assume that 95% of the biases for the modelled storm surges are encapsulated by the ± 0.036 m range, which equates to a standard error of ± 0.018 m. Next we divide the 95% confidence limits on the statistical estimates for storm surge return levels by 1.96 and add the resulting standard errors to the formula. Finally we incorporate the standard errors estimated for the joint probability sampling of tide and surge heights and use the combined error formula to evaluate a standard error for the current climate storm tide return levels. Confidence intervals for the storm tide return levels are derived from these standard errors.

As regards future storm tide return levels, we take a simple scenario-based approach to representing uncertainties in the effects of mean sea level rise and wind speed change on return levels and do not attempt to represent these uncertainties as confidence intervals. We expect the modelling and statistical fitting uncertainties associated with the current climate storm tides to be broadly applicable to storm tides for each individual future climate scenario considered. We note that an extra contribution to the storm surge modelling uncertainty arises due to the incorporation of wind speed increases. However, this will be small compared to the uncertainty associated with the changes in mean sea level and wind speed spanned by the future climate scenarios that we have considered. An analysis of this additional modelling uncertainty would therefore add little in the context of our future climate scenarios and we have chosen to neglect it.

2.7 Development of Inundation Layers

After 1 in 100 year return levels for total sea level (storm surge + tide + mean sea level rise) were evaluated across the Bass Strait region, a DEM was used to develop GIS layers identifying low-lying coastal land vulnerable to inundation (in this study we regard land potentially subject to stormtide inundation at least every 100 years on average as being vulnerable). The digital elevation data that was used in the inundation calculations was obtained from an airborne terrestrial LiDAR survey of the Victorian coast from the coastline to approximately the 10 m contour on the landward side of the coast. The inland extent of the elevation data collected along the coast is shown in Figure 5.

Five regions along the coast (also shown in Figure 5) were selected for inundation analysis on the basis that they contained extensive areas of terrain below 2 m elevation that will be potentially vulnerable to increasing sea levels in the future. Model grids were set up over these regions at 10 m horizontal resolution and the 1 in 100 year storm tide surface was interpolated to each of these grids.

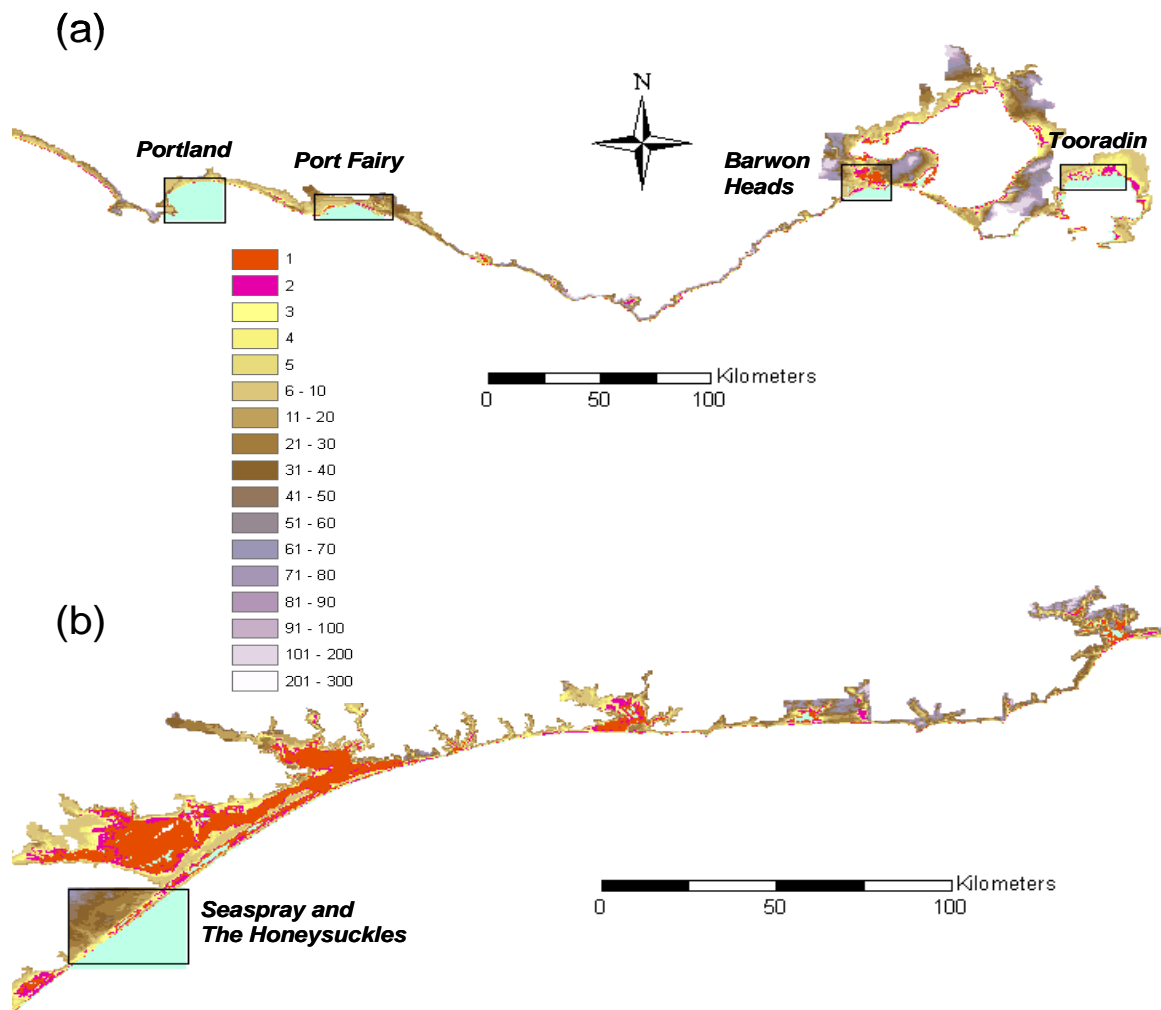


Figure 5: Digital Elevation Data in m (AHD) sourced from the Victorian Department of Sustainability and Environment's 'Future Coasts' LiDAR survey for the coastlines of western Victoria (a) and eastern Victoria (b). The five rectangular regions show areas containing extensive low-lying terrain (less than 2 m AHD) which have been selected for inundation analysis.

A simple technique was used to estimate the area likely to become inundated. Dry land points were reclassified as inundated points by carrying out sweeps across the model grid from east to west, west to east, north to south and south to north and comparing the height of the coastal sea level in the 1 in 100 year storm tide surface to the adjacent land point. If the sea level exceeds the land height, the land point is inundated to the level of the adjacent sea point.

A further check was carried out to ascertain if there were other adjacent points that could flood the point in question. For example, on a grid extending from $i = 1, ni$ in the east-west direction and $j = 1, nj$ in the north-south direction, if, on a south to north sweep of the grid (j increasing), the sea level at the point (i, j) exceeded the land height at adjacent land point $(i, j+1)$, then the land point at $(i, j+1)$ was identified as a point likely to be inundated and was provisionally assigned a water depth of the (i, j) point minus the terrain height. A check was then made on points to the left and right of the targeted point, i.e. the $(i-1, j+1)$ and $(i+1, j+1)$ points and if one or both of them were also wet, the water level of the land point at $(i, j+1)$ was then assigned the average depth of the adjacent wet points minus the terrain height.

The advantages of this simple approach are: (1) the area of inundation for a range of storm tide return levels can be easily estimated once the extreme value and joint probability analyses are complete, (2) it is computationally inexpensive to explore a range of future sea level rise scenarios and (3) the inundation can be estimated on a higher resolution grid than that used for the storm tide modelling and can be easily revised if and when more accurate terrain data become available.

However, there are also several caveats that should be noted with this simple non-dynamical approach to calculating inundation. Firstly, there is no accounting for the flood water currents and how these would be modified by friction at the terrain surface or how wind stress may increase or impede the current flow. For areas that contain tracts of low-lying land that penetrate far inland, coastal sea levels may not penetrate as far inland as indicated by this technique. There is also no accounting for the duration of the higher storm tide levels and the effect this would have on the inland penetration of inundation. If the storm tide sea levels peak for only a short period of time, then the inland penetration of flood water would be limited. However, this is a limitation only for the storm tide component of the extreme sea levels rather than the sea level rise component since the former is a transitory process while the latter is a long term change which may lead to permanent inundation of low-lying coastal terrain.

It should also be noted that there are other factors that could contribute to coastal flooding that are not considered in this study. These include the effects of waves such as wave setup and runup on the open coast (see Figure 1) and rainfall and riverine runoff, which may enhance the amount of inundation that occurs during a storm tide event. Therefore, the inundation analysis and maps shown in this study should be considered only as indicative of areas that would be vulnerable to inundation under the scenarios and storm conditions considered. They have been prepared to identify areas vulnerable to the climate change scenarios considered and to prioritise further studies and adaptation responses in the future.

3. CLIMATE CHANGE SCENARIOS FOR SEA LEVEL AND WIND SPEED

Two aspects of climate change have the potential to influence the height and frequency of extreme sea level events in the future. These are mean sea level rise and possible changes in the behaviour of the severe weather conditions responsible for storm surges. With regards to the weather conditions responsible for a storm surge, both wind speed and falling atmospheric pressure contribute to their formation. Along the Victorian coast, McInnes and Hubbert (2003) found that the effect of wind speed is much greater than that of pressure. Therefore, this study considers only the impact of possible wind speed changes due to climate change on storm surges.

The future conditions described for both mean sea level rise and wind speed change are consistent with the IPCC's Special Report on Emission Scenarios (SRES)'s A1FI scenario for the future evolution of greenhouse gas and aerosol emissions (see Nakićenović and Swart, 2000). The A1FI scenario is one of six SRES scenarios, each based on a plausible storyline of future global demographic, economic and technological change in the 21st Century. According to the A1FI storyline the global population peaks in the middle of the century, the global economy grows rapidly and continues to be reliant on fossil fuels and the introduction of new and more efficient technologies is rapid and widespread. Of the six SRES scenarios, the A1FI scenario results in the greatest rate of increase in atmospheric carbon dioxide concentrations, and, consequently, in global average surface temperature and mean sea level, over the 21st Century.

Raupach et al. (2007) report that the observed trajectory of global carbon dioxide emissions from fossil-fuel burning and industrial processes for the 2000-2006 period is close to that of the A1FI emission scenario. Furthermore, global mean sea levels are rising at a rate consistent with this scenario (Rahmstorf et al. 2007). However, it is unclear to what extent future emissions will track the A1FI scenario. A sustained decrease in the carbon intensity of Gross Domestic Product that is assumed by all of the SRES emissions scenarios has not been observed, which suggest that future emissions could exceed those of A1FI. On the other hand, the A1FI scenario takes no account of the possible future introduction of policies designed to limit greenhouse gas emissions.

Based on the current lines of evidence around climate change and possible future emissions, the Victorian Coastal Policy (2008) recommends planning for not less than 0.80 m of sea level rise by the end of the 21st Century. This level is consistent with the upper end of the range of sea level rise for the A1FI scenario. Consequently, the analysis based in this study draws upon projections of climate change that are also consistent with this scenario. In recognition of the possibility that sea levels rise may exceed that of the A1FI scenario, two additional sea level rise scenarios are also explored. These include the scenario of 1.10 m above late 20th Century mean sea level by 2100 adopted by the Netherlands Delta Committee (Vellinga, 2008) and the scenario of 1.4 m above late 20th Century mean sea level by 2100 determined by Rahmstorf (2007) using a statistical based model of sea level rise.

3.1 Sea Level Rise

Sea levels fluctuate dramatically over glacial time scales due to changes in ocean mass arising from the transfer of water between the oceans and the terrestrial landscape and due to changes in the ocean volume from variations in the ocean temperature. Between 20 thousand years ago, at the time of the last ice age, and 6000 years ago, sea level rose by over 120 metres; whereas for the 2000 years up to the start of the 19th Century, sea levels remained reasonably constant. Since the early 1800s, sea levels have been rising at an increasing rate. This is now beginning to impact coastal regions and low lying islands that have been occupied and developed during the period of relatively stable sea levels of the previous two millennia.

Global-average sea levels rose by about 0.17 m during the 20th Century (Church and White 2006) and there was a significant increase in the rate of sea level rise during the century. The average global rate of sea level rise between 1950 and 2000 was $1.8 \pm 0.3 \text{ mm yr}^{-1}$, and for the period during which satellite altimeter data are available (i.e. from 1993), the rate exceeds 3 mm yr^{-1} (Church and White 2006). The observed rate of global sea-level rise since 1990 corresponds to the upper bound of estimates for the SRES A1FI emission scenario in the IPCC's Third Assessment Report (IPCC, 2001) projections (Rahmstorf et al., 2007), causing concern that values of sea level rise derived from global climate model simulations may be underestimating one or more of the contributions to sea level rise.

Future sea level rise projections provided by the IPCC's Fourth Assessment Report (IPCC, 2007) give the likely range of values for sea-level rise over the 1990-2095 period as 0.18 to 0.79 m. This range includes several sources of uncertainty. These are the uncertainty around future emissions of greenhouse gases represented by the SRES scenarios (Nakićenović and Swart, 2000), the uncertainty around the thermal expansion of the world's oceans in response to global warming, the uncertainty in the amount of sea level rise due to the melting of glaciers and ice sheets and the additional uncertainty related to the potential for ice flow from Greenland and Antarctica to accelerate. Hunter (2009) scaled the IPCC (2007) sea level rise figures to earlier decades throughout the 21st Century. The Victorian Coastal Strategy (2008) has adopted a precautionary approach to planning for sea level rise (see <http://www.vcc.vic.gov.au/vcs.htm>) and recommends that a sea level rise value of not less than 0.8 m by 2100 should be considered for coastal planning and development, which is approximately equal to the high-end of the IPCC (2007) sea level rise estimates. Since the release of the IPCC (2007) report, other sea level rise and coastal impact assessments have been undertaken that put forward alternative sea level rise scenarios for 2100. For example, based on a simple statistical model, Rahmstorf (2007) suggests a likely range of values for sea-level rise over the 1990-2100 period of 0.5 to 1.4 m. A report prepared for the Dutch Delta Committee, which assesses post- Fourth Assessment Report publications on the impacts of recent warming trends on ice sheet dynamics, derives an upper bound of sea level rise of 1.1 m by 2100 (Vellinga, 2008). These additional scenarios have also been considered in the present study and are summarised in Table 4.

Climate change scenarios 1, 2 and 4 described in Table 4 incorporate sea level rise only. To estimate future storm tide return levels for these scenarios, the relevant estimate of sea level rise was simply added to the storm tide return levels estimated for current climate conditions. This approach makes the assumption, which is expected to be reasonable for much of the Victorian coastline, that sea level rise will have little effect on tide heights. However, we note

that an increase in mean sea level may increase the tidal range within Port Phillip Bay due to reduced frictional attenuation of tidal flows through the shallow entrance to the bay. The reader is referred to McInnes et al (2009c), a high resolution study of the effect of climate change on extreme sea levels in Port Phillip Bay, for further discussion of this effect.

Table 4: Climate change scenarios considered in the present study. Scenario 1 considers the IPCC (2007) high scenario for mean sea level, scenario 2 combines the high sea level rise scenario with the equivalent high annual averaged wind speed change averaged over Bass Strait from CSIRO and Australian Bureau of Meteorology (2007). Scenario 3 considers the upper sea level rise scenario developed for the Netherlands Delta Committee and scenario 4 considers the upper sea level scenario proposed by Rahmstorf (2007). Note that asterisked values were not investigated in the present study.

Future climate scenario			2030	2070	2100
1	IPCC 2007 A1FI scenario Hunter (2009)	Sea level rise (m)	0.15	0.47	0.82
2	IPCC 2007 A1FI scenario in combination with 'high' wind speed scenario	Sea level rise (m)	0.15	0.47	0.82
		Wind speed increase (%)	4	13	19
3	Sea level rise based on Netherlands Delta Committee Vellinga (2008)	Sea level rise (m)	0.20*	0.70*	1.10
4	Rahmstorf (2007) upper estimate	Sea level rise (m)	0.23*	0.74*	1.40

3.2 Wind Speed

The largely westerly to southerly winds associated with the passage of cold fronts have been found to be the main driver of storm surges along the Victorian coast (McInnes and Hubbert, 2003; McInnes et al., 2005). Therefore, the impact of future wind speed changes on storm surges were explored in this study. Projections of future wind speed changes were obtained from a recent report giving climate change projections for Australia (CSIRO and Australian Bureau of Meteorology, 2007) (see <http://www.climatechangeinaustralia.gov.au/>). In this report, the method described by Watterson (2008) is used to develop projections of various climate variables from the output of set of climate model simulations that were undertaken for the IPCC Fourth Assessment Report (IPCC, 2007). Gridded probabilistic projections for future changes in annual average wind speed are provided for the Australian region for three of the SRES emission scenarios, including the A1FI scenario. To be consistent with the high-end A1FI estimates of sea level rise used in this study, the high (90th percentile) estimates for changes in annual average wind speed for the A1FI emissions scenario from the projections report were used. The gridded changes were averaged spatially over the region bounded by 140 – 150° E and 38 – 41°S to give the values shown in Table 4. These values are presented as a percentage wind speed change relative to the period 1980 to 1999. It should be noted that, because of the large uncertainties in wind speed change in this region as represented by the set of Fourth Assessment Report climate models, the Australian projections did not preclude the possibility of future decreases in annual average wind speed in Bass Strait.

McInnes et al (2005b) noted that storm surge heights in Bass Strait respond linearly to changes in wind speed, with a 1% increase in wind speed corresponding, approximately, to a 2% increase in storm surge height. This property was used in this study to estimate future storm tide return levels for climate change scenario 2 described in Table 4, which incorporates both wind speed increase and sea level rise. The effect of wind speed increase was accounted for by simply increasing the storm surge heights estimated for current climate conditions by a percentage equal to twice the relevant percentage wind speed increase prior to input to the JPM. The effect of sea level rise was then accounted for by simply adding the relevant estimate of sea level rise to the resulting storm tide return levels.

4. EXTREME SEA LEVEL ANALYSIS

Return levels are presented for the storm surge component of sea level only prior to the presentation of return levels for total sea levels comprising both the surge and tide components. It should be noted that the methodology developed in this study, as well as the resolution of the hydrodynamic models and bathymetric and atmospheric data sets used, have been guided by the desire to provide data for the entire Victorian coast within the limitations of the available computing resources. It is possible that higher resolution studies of sections of the coastline using different methodologies and data sets may yield different return levels.

4.1 Storm Surge Return Levels

The spatial pattern of 1 in 100 year storm surge heights for the Victorian coast under late 20th Century climate conditions is shown in Figure 6. Values range between 0.5 and 1.0 m along the open coastline. The lowest coastal values occur in the west. At Portland, the 1 in 100 storm surge level is between 0.5 and 0.6 m. The highest levels, between 0.9 and 1.0 m, occur along the stretch of coastline between Wilson's Promontory and Lakes Entrance that includes Ninety Mile Beach. Similar high levels occur on the eastern side of Western Port Bay. Note that in Figure 6 and in the estimation of surge height probabilities that are input into the JPM, data from related high resolution studies was used to supplement the 1 km resolution data in Port Phillip Bay, Western Port Bay, Corner Inlet and the region of the Gippsland Lakes, (McInnes et al., 2006, 2008, 2009c).

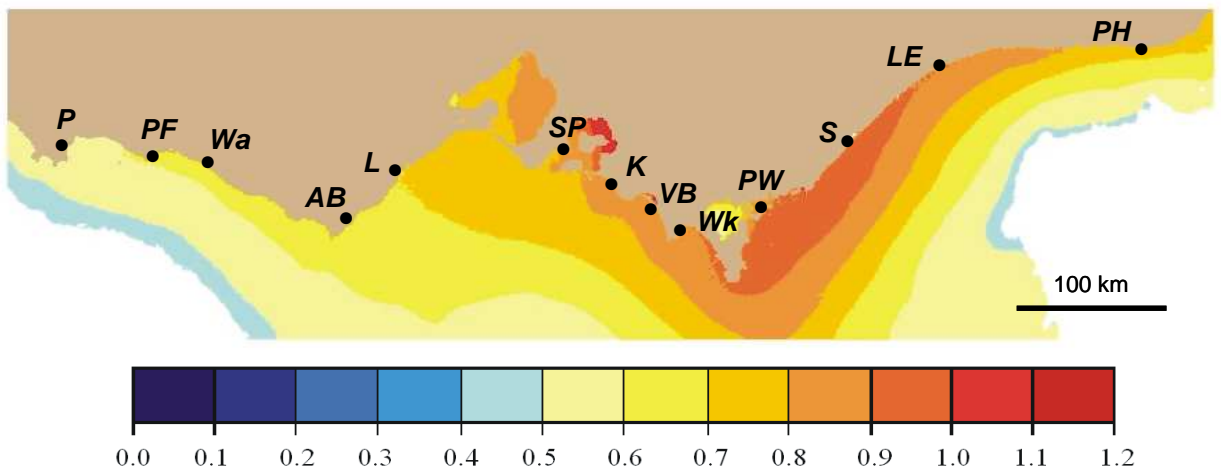


Figure 6: The spatial pattern of 1 in 100 year storm surge heights for the Victorian coast under late 20th Century climate conditions. Note that these do not include a tidal component. Values are in metres relative to late 20th Century mean sea level. P=Portland, PF=Port Fairy, Wa=Warrnambool, AB=Apollo Bay, L=Lorne, SP=Stony Point, K=Kilcunda, VB=Venus Bay, Wk=Walkerville, PW=Port Welshpool, S=Seaspray, LE=Lakes Entrance, PH=Point Hicks.

Table 5: Storm surge height return levels for selected Victorian locations (see Figure 6) under current climate conditions and climate change scenarios as indicated in Table 4. All values are in metres relative to late 20th Century mean sea level. Values for Port Welshpool and Lakes Entrance are from McInnes et al. (2009), in which high resolution modelling was undertaken. Higher resolution studies of sections of the coastline using different methodologies may yield different return levels than this study of the entire Victorian coast.

Location	Period (yrs)	Current Climate		2030			2070			2100			
				1	2	3	1	2	3	1	2	3	4
Portland	10	0.51	±0.04	0.66	0.70	0.71	0.98	1.11	1.21	1.33	1.52	1.61	1.91
	20	0.52	±0.04	0.67	0.71	0.72	0.99	1.13	1.22	1.34	1.54	1.62	1.92
	50	0.54	±0.04	0.69	0.73	0.74	1.01	1.15	1.24	1.36	1.56	1.64	1.94
	100	0.55	±0.05	0.70	0.74	0.75	1.02	1.16	1.25	1.37	1.57	1.65	1.95
Port Fairy	10	0.56	±0.04	0.71	0.75	0.76	1.03	1.17	1.26	1.38	1.59	1.66	1.96
	20	0.57	±0.04	0.72	0.77	0.77	1.04	1.19	1.27	1.39	1.61	1.67	1.97
	50	0.59	±0.05	0.74	0.79	0.79	1.06	1.21	1.29	1.41	1.64	1.69	1.99
	100	0.60	±0.05	0.75	0.80	0.80	1.07	1.23	1.30	1.42	1.65	1.70	2.00
Warrnambool	10	0.59	±0.04	0.74	0.79	0.79	1.06	1.22	1.29	1.41	1.64	1.69	1.99
	20	0.61	±0.05	0.76	0.81	0.81	1.08	1.24	1.31	1.43	1.66	1.71	2.01
	50	0.63	±0.05	0.78	0.83	0.83	1.10	1.26	1.33	1.45	1.69	1.73	2.03
	100	0.64	±0.05	0.79	0.84	0.84	1.11	1.28	1.34	1.46	1.70	1.74	2.04
Apollo Bay	10	0.62	±0.04	0.77	0.82	0.82	1.09	1.25	1.32	1.44	1.67	1.72	2.02
	20	0.64	±0.05	0.79	0.84	0.84	1.11	1.27	1.34	1.46	1.70	1.74	2.04
	50	0.66	±0.05	0.81	0.86	0.86	1.13	1.30	1.36	1.48	1.73	1.76	2.06
	100	0.67	±0.05	0.82	0.87	0.87	1.14	1.31	1.37	1.49	1.74	1.77	2.07
Lorne	10	0.66	±0.04	0.81	0.86	0.86	1.13	1.30	1.36	1.48	1.73	1.76	2.06
	20	0.68	±0.05	0.83	0.88	0.88	1.15	1.32	1.38	1.50	1.75	1.78	2.08
	50	0.70	±0.05	0.85	0.90	0.90	1.17	1.35	1.40	1.52	1.78	1.80	2.10
	100	0.71	±0.05	0.86	0.92	0.91	1.18	1.36	1.41	1.53	1.80	1.81	2.11
Stony Point	10	0.74	±0.05	0.89	0.95	0.94	1.21	1.40	1.44	1.56	1.84	1.84	2.14
	20	0.77	±0.05	0.92	0.98	0.97	1.24	1.44	1.47	1.59	1.88	1.87	2.17
	50	0.80	±0.06	0.95	1.01	1.00	1.27	1.48	1.50	1.62	1.92	1.90	2.20
	100	0.82	±0.06	0.97	1.04	1.02	1.29	1.50	1.52	1.64	1.95	1.92	2.22
Kilcunda	10	0.75	±0.05	0.90	0.96	0.95	1.22	1.42	1.45	1.57	1.86	1.85	2.15
	20	0.78	±0.05	0.93	0.99	0.98	1.25	1.45	1.48	1.60	1.90	1.88	2.18
	50	0.81	±0.06	0.96	1.02	1.01	1.28	1.49	1.51	1.63	1.94	1.91	2.21
	100	0.83	±0.07	0.98	1.04	1.03	1.30	1.51	1.53	1.65	1.96	1.93	2.23
Venus Bay	10	0.77	±0.05	0.92	0.98	0.97	1.24	1.44	1.47	1.59	1.88	1.87	2.17
	20	0.80	±0.05	0.95	1.01	1.00	1.27	1.48	1.50	1.62	1.92	1.90	2.20
	50	0.83	±0.06	0.98	1.05	1.03	1.30	1.52	1.53	1.65	1.97	1.93	2.23
	100	0.85	±0.07	1.00	1.07	1.05	1.32	1.54	1.55	1.67	1.99	1.95	2.25
Walkerville	10	0.77	±0.05	0.92	0.98	0.97	1.24	1.44	1.47	1.59	1.89	1.87	2.17
	20	0.80	±0.06	0.95	1.02	1.00	1.27	1.48	1.50	1.62	1.93	1.90	2.20
	50	0.84	±0.07	0.99	1.05	1.04	1.31	1.52	1.54	1.66	1.98	1.94	2.24
	100	0.86	±0.07	1.01	1.08	1.06	1.33	1.55	1.56	1.68	2.00	1.96	2.26
Port Welshpool	10	0.63	±0.06	0.78	0.83	0.83	1.10	1.26	1.33	1.45	1.68	1.73	2.03
	20	0.66	±0.07	0.81	0.86	0.86	1.13	1.30	1.36	1.48	1.73	1.76	2.06
	50	0.70	±0.08	0.85	0.91	0.90	1.17	1.35	1.40	1.52	1.79	1.80	2.10
	100	0.72	±0.09	0.87	0.93	0.92	1.19	1.38	1.42	1.54	1.81	1.82	2.12
Seaspray	10	0.83	±0.06	0.98	1.04	1.03	1.30	1.51	1.53	1.65	1.96	1.93	2.23
	20	0.86	±0.07	1.01	1.08	1.06	1.33	1.55	1.56	1.68	2.01	1.96	2.26
	50	0.90	±0.08	1.05	1.13	1.10	1.37	1.61	1.60	1.72	2.07	2.00	2.30
	100	0.93	±0.10	1.08	1.15	1.13	1.40	1.64	1.63	1.75	2.10	2.03	2.33
Lakes Entrance	10	0.59	±0.04	0.74	0.79	0.79	1.06	1.21	1.29	1.41	1.63	1.69	1.99
	20	0.62	±0.04	0.77	0.82	0.82	1.09	1.25	1.32	1.44	1.68	1.72	2.02
	50	0.64	±0.05	0.79	0.84	0.84	1.11	1.28	1.34	1.46	1.70	1.74	2.04
	100	0.65	±0.05	0.80	0.85	0.85	1.12	1.29	1.35	1.47	1.72	1.75	2.05
Point Hicks	10	0.70	±0.05	0.85	0.91	0.90	1.17	1.35	1.40	1.52	1.79	1.80	2.10
	20	0.72	±0.05	0.87	0.93	0.92	1.19	1.38	1.42	1.54	1.82	1.82	2.12
	50	0.75	±0.06	0.90	0.95	0.95	1.22	1.41	1.45	1.57	1.85	1.85	2.15
	100	0.76	±0.07	0.91	0.97	0.96	1.23	1.43	1.46	1.58	1.87	1.86	2.16

Storm surge heights for the 10, 20, 50 and 100 year return periods are presented in Table 5 for selected locations along the Victorian coast under late 20th Century climate conditions as well as for the climate change scenarios presented in Table 4. The 95% confidence intervals presented in the table represent uncertainties associated with imperfections in the storm surge simulations and the statistical fits to the extreme surge heights .

4.2 Storm Tide Return Levels

A storm tide is the combination of a storm surge with the astronomical tide and represents the actual sea levels that are experienced at the coast during a storm event. The spatial pattern of 1 in 100 year storm tide heights for the Victorian coast under late 20th Century climate conditions is shown in Figure 7a. The highest coastal values, in excess of 2 m, occur in and around Western Port Bay and values of 1.8 to 2.0 m extend from just west of Port Phillip Bay to Wilson's Promontory. These high values are the result of a large contribution from both storm surges and astronomical tides. In Port Phillip Bay, the low storm tide heights of 1.0 to 1.2 m are due to the strong attenuation of the tides across the entrance to the bay. It is noteworthy that the 1 in 100 year storm tide heights in the west are lower than the Netherland Delta Committee and Rahmstorf (2007) estimates of sea level rise for 2100 (see Table 4). If these estimates prove to be accurate, then by 2100 mean sea level will lie above the current 1 in 100 year storm tide height.

Storm tide heights for the 10, 20, 50 and 100 year return periods are presented in Table 6 for selected locations along the Victorian coast under late 20th Century climate conditions as well as for the climate change scenarios presented in Table 4. The 95% confidence intervals presented in the table represent uncertainties associated with imperfections in the tide simulations, imperfections in the storm surge simulations, the statistical fits to the extreme surge heights and the combination of tide and surge heights. We note that the storm tide return levels presented in this study differ from those in McInnes et al. (2009). This is because modelled tides were used in this study whereas McInnes et al. (2009) sourced tidal constituent data from tide gauge observations.

By comparing storm tide return levels for scenario 2, which considers both wind speed change and sea level rise, with those for scenario 1, which only considers sea level rise, we can assess the relative contributions of wind speed increases and sea level rise to changes in extreme sea levels. For return periods between 10 and 100 years, storm tide return levels for 2030 for scenario 2 are 0.04-0.09 m higher than those for scenario 1. For 2070 and 2100 the differences between the scenario 2 and scenario 1 return levels are 0.11-0.21 m and 0.16-0.31 m respectively. These results indicate that, for the high-end A1FI sea level rise estimates considered, the contribution of consistent high-end estimates of wind speed increase to increases in extreme storm surge heights is considerably smaller, by a factor of more than two, than the contribution of sea level rise. It therefore seems likely that climate change will have a greater impact on extreme storm surge heights through sea level rise than through wind speed changes. It follows that sea levels currently attained only during severe storms will be reached during much less extreme conditions in the future.

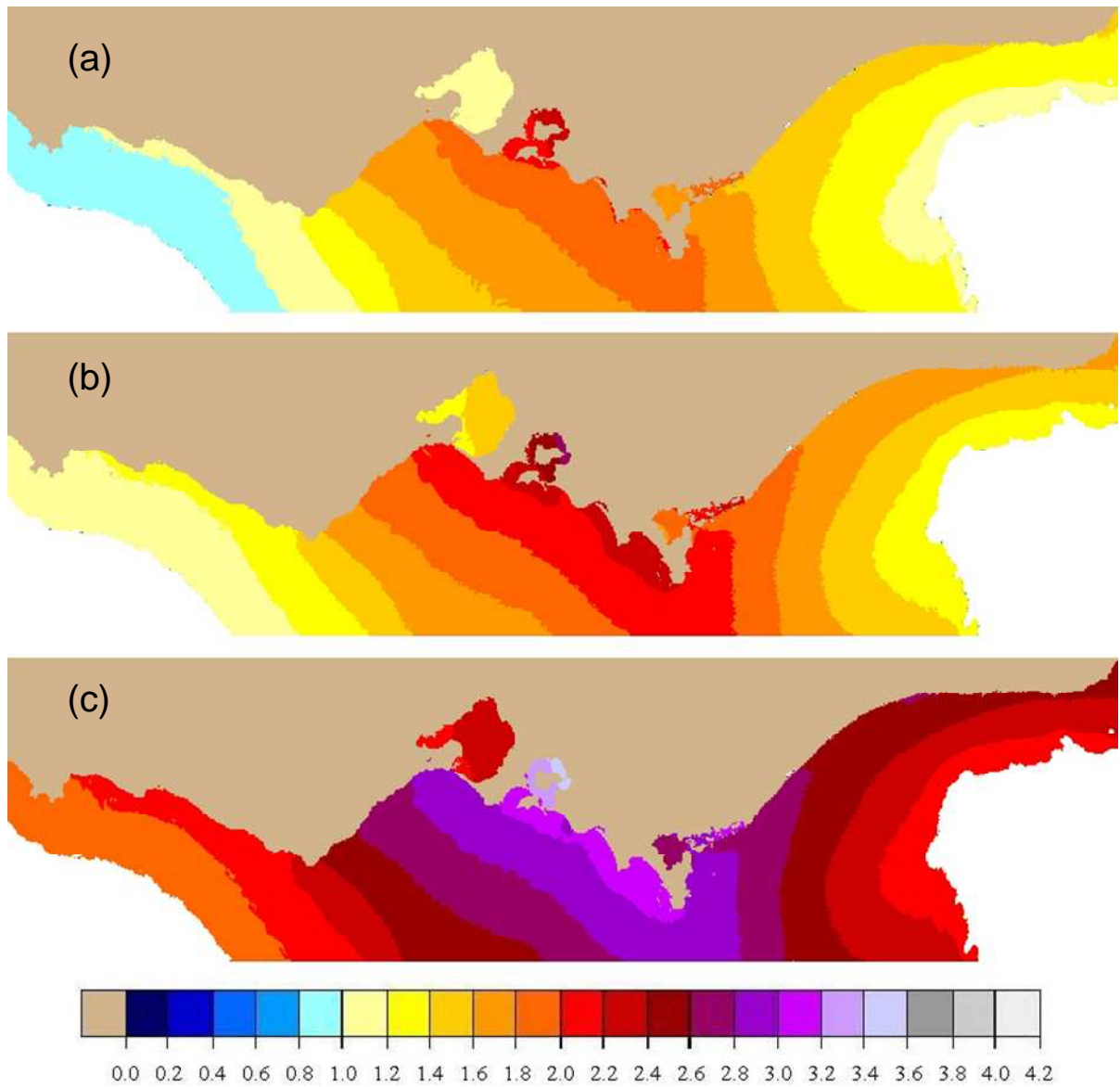


Figure 7: The spatial pattern of 1 in 100 year storm tide heights for the Victorian coast under (a) late 20th Century climate conditions, (b) including scenario 2 wind speed increases for 2100 without sea level rise , (c) for scenario 2 in 2100. Values are in metres relative to late 20th Century mean sea level.

Table 6: Storm tide height return levels for selected Victorian locations (see Figure 6) under current climate conditions and climate change scenarios as indicated in Table 4. All values are in metres relative to late 20th Century mean sea level. Values for Port Welshpool and Lakes Entrance are from McInnes et al. (2009), in which high resolution modelling was undertaken. Higher resolution studies of sections of the coastline using different methodologies may yield different return levels than this study of the entire Victorian coast.

Location	Period (yrs)	Current Climate	2030			2070			2100			
			1	2	3	1	2	3	1	2	3	4
Portland	10	0.79 ±0.09	0.94	1.00	0.99	1.26	1.39	1.49	1.61	1.81	1.89	2.19
	20	0.89 ±0.09	1.04	1.08	1.09	1.36	1.47	1.59	1.71	1.88	1.99	2.29
	50	0.97 ±0.09	1.12	1.17	1.17	1.44	1.57	1.67	1.79	1.97	2.07	2.37
	100	1.01 ±0.10	1.16	1.22	1.21	1.48	1.61	1.71	1.83	2.05	2.11	2.41
Port Fairy	10	0.83 ±0.08	0.98	1.03	1.03	1.30	1.44	1.53	1.65	1.86	1.93	2.23
	20	0.93 ±0.08	1.08	1.13	1.13	1.40	1.52	1.63	1.75	1.94	2.03	2.33
	50	1.01 ±0.10	1.16	1.21	1.21	1.48	1.61	1.71	1.83	2.03	2.11	2.41
	100	1.05 ±0.12	1.20	1.25	1.25	1.52	1.67	1.75	1.87	2.09	2.15	2.45
Warrnambool	10	0.85 ±0.12	1.00	1.05	1.05	1.32	1.46	1.55	1.67	1.89	1.95	2.25
	20	0.95 ±0.12	1.10	1.14	1.15	1.42	1.54	1.65	1.77	1.97	2.05	2.35
	50	1.03 ±0.13	1.18	1.23	1.23	1.50	1.64	1.73	1.85	2.05	2.13	2.43
	100	1.06 ±0.14	1.21	1.27	1.26	1.53	1.69	1.76	1.88	2.13	2.16	2.46
Apollo Bay	10	1.10 ±0.12	1.25	1.30	1.30	1.57	1.71	1.80	1.92	2.13	2.20	2.50
	20	1.23 ±0.12	1.38	1.43	1.43	1.70	1.82	1.93	2.05	2.25	2.33	2.63
	50	1.34 ±0.12	1.49	1.55	1.54	1.81	1.95	2.04	2.16	2.36	2.44	2.74
	100	1.42 ±0.13	1.57	1.63	1.62	1.89	2.04	2.12	2.24	2.46	2.52	2.82
Lorne	10	1.32 ±0.13	1.47	1.52	1.52	1.79	1.94	2.02	2.14	2.35	2.42	2.72
	20	1.46 ±0.13	1.61	1.67	1.66	1.93	2.06	2.16	2.28	2.50	2.56	2.86
	50	1.59 ±0.14	1.74	1.81	1.79	2.06	2.22	2.29	2.41	2.63	2.69	2.99
	100	1.69 ±0.16	1.84	1.91	1.89	2.16	2.33	2.39	2.51	2.74	2.79	3.09
Stony Point	10	1.62 ±0.19	1.77	1.83	1.82	2.09	2.25	2.32	2.44	2.68	2.72	3.02
	20	1.79 ±0.20	1.94	2.00	1.99	2.26	2.40	2.49	2.61	2.85	2.89	3.19
	50	1.94 ±0.21	2.09	2.17	2.14	2.41	2.61	2.64	2.76	3.00	3.04	3.34
	100	2.08 ±0.22	2.23	2.30	2.28	2.55	2.73	2.78	2.90	3.14	3.18	3.48
Kilcunda	10	1.54 ±0.10	1.69	1.76	1.74	2.01	2.19	2.24	2.36	2.61	2.64	2.94
	20	1.70 ±0.10	1.85	1.92	1.90	2.17	2.33	2.40	2.52	2.77	2.80	3.10
	50	1.85 ±0.10	2.00	2.08	2.05	2.32	2.50	2.55	2.67	2.92	2.95	3.25
	100	1.94 ±0.12	2.09	2.18	2.14	2.41	2.61	2.64	2.76	3.03	3.04	3.34
Venus Bay	10	1.54 ±0.10	1.69	1.76	1.74	2.01	2.19	2.24	2.36	2.63	2.64	2.94
	20	1.70 ±0.10	1.85	1.93	1.90	2.17	2.33	2.40	2.52	2.78	2.80	3.10
	50	1.86 ±0.10	2.01	2.09	2.06	2.33	2.51	2.56	2.68	2.93	2.96	3.26
	100	1.96 ±0.12	2.11	2.20	2.16	2.43	2.64	2.66	2.78	3.06	3.06	3.36
Walkerville	10	1.57 ±0.10	1.72	1.78	1.77	2.04	2.21	2.27	2.39	2.65	2.67	2.97
	20	1.73 ±0.10	1.88	1.94	1.93	2.20	2.37	2.43	2.55	2.80	2.83	3.13
	50	1.89 ±0.10	2.04	2.13	2.09	2.36	2.53	2.59	2.71	2.95	2.99	3.29
	100	1.98 ±0.12	2.13	2.22	2.18	2.45	2.65	2.68	2.80	3.08	3.08	3.38
Port Welshpool	10	1.35 ±0.12	1.50	1.55	1.55	1.82	1.96	2.05	2.17	2.38	2.45	2.75
	20	1.46 ±0.12	1.61	1.66	1.66	1.93	2.06	2.16	2.28	2.49	2.56	2.86
	50	1.57 ±0.12	1.72	1.78	1.77	2.04	2.20	2.27	2.39	2.61	2.67	2.97
	100	1.63 ±0.14	1.78	1.84	1.83	2.10	2.27	2.33	2.45	2.68	2.73	3.03
Seaspray	10	1.22 ±0.12	1.37	1.42	1.42	1.69	1.87	1.92	2.04	2.33	2.32	2.62
	20	1.32 ±0.12	1.47	1.54	1.52	1.79	1.98	2.02	2.14	2.44	2.42	2.72
	50	1.43 ±0.12	1.58	1.66	1.63	1.90	2.09	2.13	2.25	2.53	2.53	2.83
	100	1.50 ±0.14	1.65	1.73	1.70	1.97	2.18	2.20	2.32	2.64	2.60	2.90
Lakes Entrance	10	0.81 ±0.09	0.96	1.01	1.01	1.28	1.42	1.51	1.63	1.85	1.91	2.21
	20	0.89 ±0.09	1.04	1.09	1.09	1.36	1.48	1.59	1.71	1.90	1.99	2.29
	50	0.98 ±0.09	1.13	1.18	1.18	1.45	1.58	1.68	1.80	2.01	2.08	2.38
	100	1.04 ±0.10	1.19	1.24	1.24	1.51	1.66	1.74	1.86	2.09	2.14	2.44
Point Hicks	10	1.11 ±0.13	1.26	1.32	1.31	1.58	1.75	1.81	1.93	2.19	2.21	2.51
	20	1.22 ±0.14	1.37	1.43	1.42	1.69	1.84	1.92	2.04	2.27	2.32	2.62
	50	1.31 ±0.14	1.46	1.53	1.51	1.78	1.95	2.01	2.13	2.38	2.41	2.71
	100	1.36 ±0.16	1.51	1.59	1.56	1.83	2.01	2.06	2.18	2.45	2.46	2.76

Figure 8 illustrates the impact that the various climate change scenarios will have on return periods at three locations along the Victorian coast. The significant differences between the contributions of sea level rise and wind speed increase to increases in storm tide return levels are clearly evident. The figure also shows how storm tides of the height currently experienced on average only once every 100 years will be experienced more frequently in the future. It should be noted, however, that since this effect is mainly due to sea level rise, not all storm tides of the current 1 in 100 year level will be accompanied by particularly severe storms. At Portland, a storm tide of the height of the current 100-year return level, 1.01 m, may occur every 20 years on average by 2030. By 2070 sea level rise alone may result in a 1.01 m event occurring with an average recurrence interval of less than 3 years and an increase in wind speed may further decrease the return period to less than 2 years. By 2100, under any of the climate change scenarios considered, such an event would be experienced at least once per year on average. At Stony Point, the current 100 year return level, 2.08 m, may be exceeded every 30 years on average by 2030. By 2070 sea level rise alone may result in a 2.08 m event occurring with an average recurrence interval of 8 years and an increase in wind speed may further decrease the return period to 5 years. By 2100, under any of the climate change scenarios considered, such an event would be experienced at least once every 1.5 years on average. At Port Welshpool, a storm tide of 1.63 m, the current 100-year return level, may become a 1 in 20 year event by 2030, a 1 in 3 year event by 2070 and a sub-annual event by 2100.

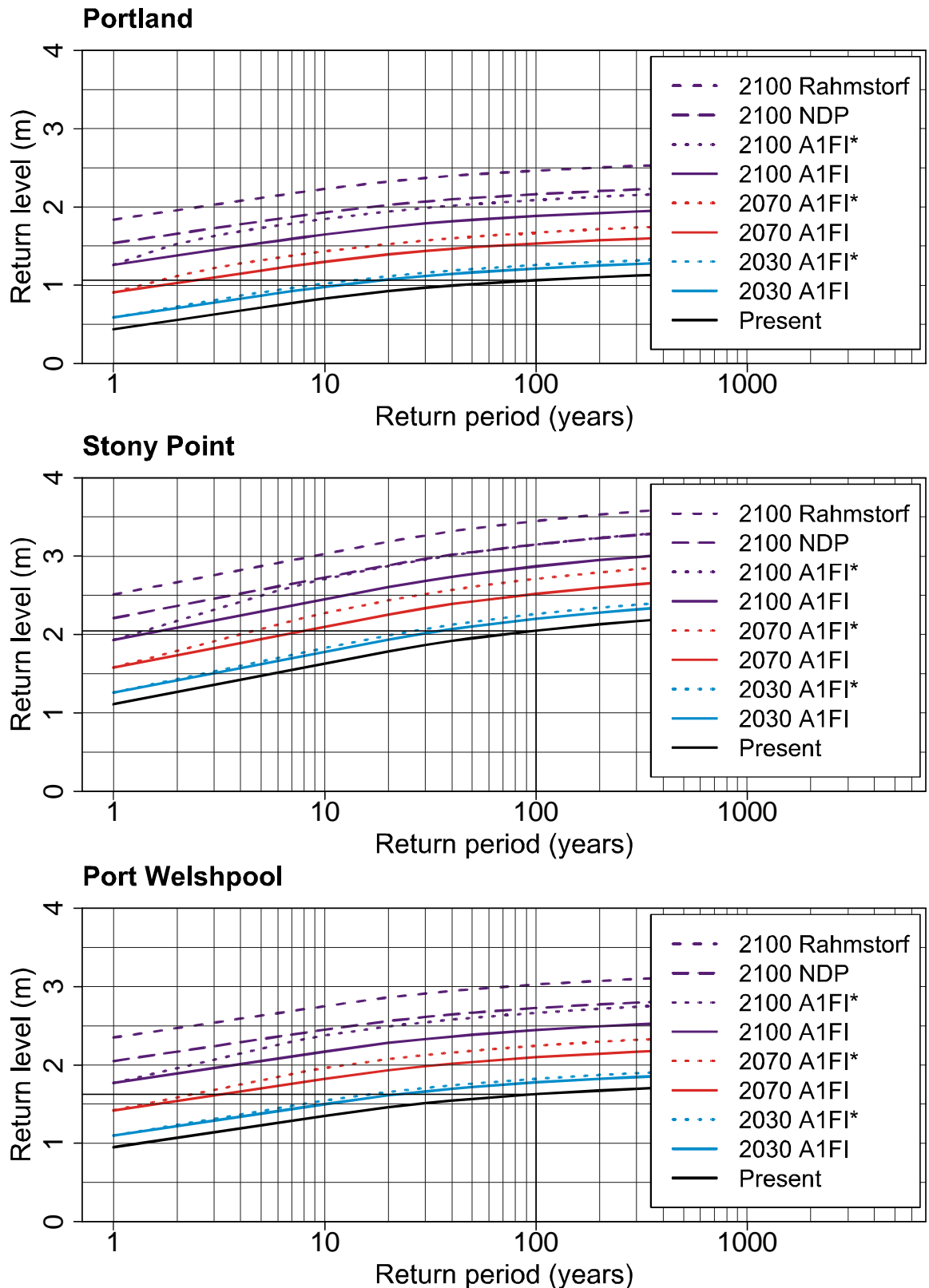


Figure 8: Storm tide height return period curves for selected Victorian locations under current climate conditions and climate change scenarios as indicated in Table 4. Note that * denotes scenarios that incorporate wind speed changes. Note that the curves for Port Welshpool have been obtained from McInnes et al. (2009), in which high resolution modelling of this location was undertaken.

5. INUNDATION AND EXPOSURE ANALYSIS

The previous section described increases in storm tide return levels for the Victorian coast under various future climate change scenarios. The impact of associated increases in coastal inundation will depend on the location of coastal assets and the topography of coastal terrain. In this section, a simple method is used to identify coastal land that is vulnerable to inundation by extreme sea levels under current climate conditions and the climate change scenarios described in Table 4. Property and transport databases are used to investigate changes in the exposure of land parcels under the climate change scenarios considered.

Five regions along the Victorian coast were selected for inundation and exposure analysis on the basis that they contained extensive areas of terrain below 2 m elevation: Portland, Port Fairy, Barwon Heads, Tooradin and Seaspray. The 1 in 100 year storm tide surfaces for the current climate and each of the climate change scenarios were interpolated to a 10 m grid set up over each region of interest. Inundation depths were evaluated using the technique described in section 2.7 and imported into a geographic information system (ARCGIS 9.3) as 10 m gridded data layers using Geographic Coordinate System: GCS_GDA_1994, Datum: D_GDA_1994 and a Transverse Mercator Projected Coordinate System: GDA_1994_MGA_Zone_54 and GDA_1994_MGA_Zone_55. The layers were converted to a vector polygon format for subsequent analysis. This included evaluating the intersection of the inundated areas with Vicmap property and transport data bases supplied by the Department of Sustainability and Environment.

In this section results for each of the five regions selected for inundation and exposure analysis are discussed in turn. The inundation layers for the current climate and a selection of climate change scenarios (scenario 1 for 2030, 2070 and 2100 and scenarios 3 and 4 for 2100 only) are presented. Tables summarising the exposure of land parcels and roadways to inundation for the current climate and a selection of climate change scenarios (scenario 1 and 2 for 2030, 2070 and 2100 and scenarios 3 and 4 for 2100 only) are also presented. For the sake of brevity, inundation and exposure information has not been presented for all of the climate change scenarios and future years in Table 4. Similarly, the text in this section seeks to highlight key features of future changes in the vulnerability of coastal land and assets to inundation and is not intended as an exhaustive discussion of every climate change scenario and future year in Table 4. Hence, though it is recognised that wind speed increases will have a small additional impact on inundation and exposure (which can be gauged by comparing the data given for scenarios 1 and 2 in the tables in this section) the discussion is confined to the effects of sea level rise only.

5.1 Portland

The coastline in the Portland region is characterised by hardrock basalt cliffs to the south of Portland and soft rock cliffs stretching from Portland township north to Dutton Way and transitioning to eastward-running dune formations (Port of Melbourne Authority, 1992) (Figure 9a).

The Portland region shows minimal inundation, amounting to less than 1 km² of land, under current climate 1 in 100 year storm tide conditions (Table 7). The impact of sea level rise on inundation associated with a 1 in 100 year storm tide is small until after 2070, scenario 1 adding less than 1 km² to the total area vulnerable to inundation. By 2100 the sea level rise estimates considered result in a doubling to tripling of the area vulnerable to inundation. The areas most affected are the foreshore regions around Portland Harbour and Nuns Beach to the north of the breakwater (Figure 9b). Also vulnerable are the lower reaches of the Surry River (Figure 9c), where low-lying terrain to the east of the river and in the vicinity of Caravan Park Road to the west of the river become vulnerable to inundation. Of the climate change scenarios considered, scenario 1 has the least impact. Under this scenario the total number of land parcels vulnerable to inundation increases by 25%, from 168 parcels under current climate conditions to 210 parcels for 2100, and the length of exposed roadway increases by approximately 50%. Under scenario 4, which has the greatest impact of the scenarios considered, the total number of land parcels vulnerable to inundation increases by 60% and the length of exposed roadway approximately triples.

Table 7: Summary of the exposure of land parcels and roadways in the Portland region to inundation under current climate conditions and various climate change scenarios.

Year	Scenario	Sea level rise m	Wind speed change %	Area of inundation km ²	Exposed land parcels	Exposed roadways km
Current climate		0	-	0.8	168	5.1
2030	1	0.15	-	1.0	178	5.1
	2	0.15	4	1.0	189	5.1
2070	1	0.47	-	1.3	180	6.1
	2	0.47	13	1.5	192	6.8
2100	1	0.82	-	1.7	210	7.5
	2	0.82	19	2.1	220	9.2
	3	1.10	-	2.0	228	9.7
	4	1.40	-	2.5	272	15.6

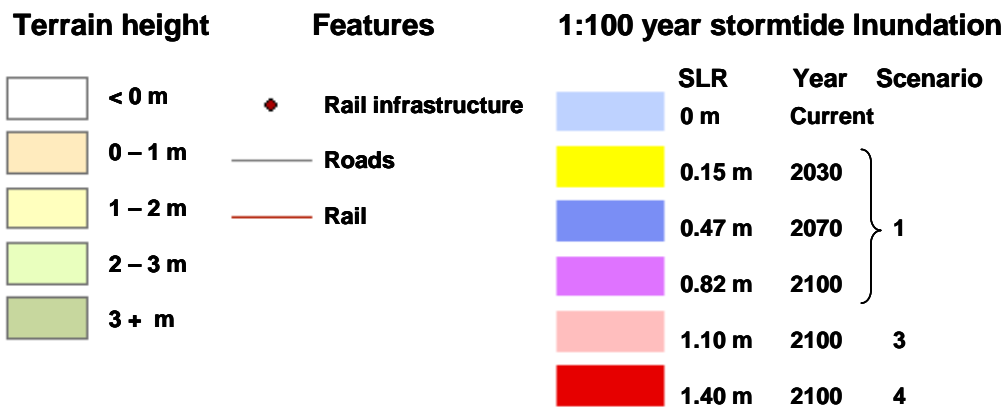


Figure 9: Land vulnerable to inundation during a 1 in 100 year storm tide under current climate conditions and various scenarios of future sea level rise for (a) the Portland region (b) Portland Harbour and (c) Surry River.

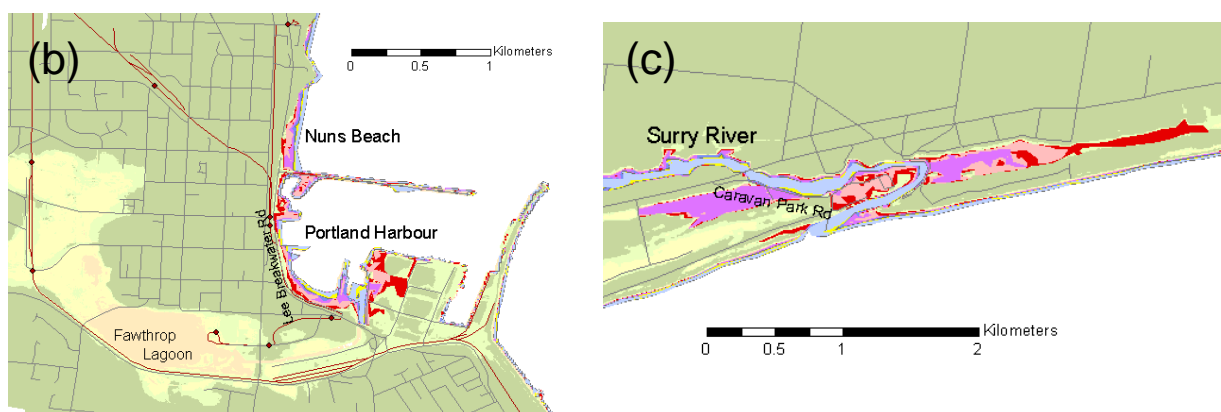


Figure 9: Continued.

5.2 Port Fairy

The Port Fairy analysis region extends from Port Fairy in the west to the western half of Warrnambool in the east (Figure 10a). The coastline in this region consists of beach backed by semi-vegetated dunes with local outcropping of basalt reefs (Port of Melbourne Authority, 1992). At Port Fairy itself, the dune system is backed by Belfast Lough, which connects to the sea via the Moyne River (Figure 10b). At Warrnambool, Lake Pertobe lies at the back of a well vegetated dune system fronting Lady Bay. Further to the west, a narrow dune system forms a barrier between the ocean and Kelly Swamp (Figure 10c).

Under current climate 1 in 100 year storm tide conditions, inundation may occur along the Moyne River and Belfast Lough at Port Fairy and along the lower reaches of the Merri River at Warrnambool. By 2030, sea level rise has a small additional effect on inundation along the banks of the Merri and Moyne Rivers and Belfast Lough, scenario 1 adding less than 1 km² to the total area vulnerable to inundation. A larger impact on inundation is seen by 2070, with extensive inundation occurring around Belfast Lough and in low-lying swamp land adjacent to the Merri River. Under scenario 1, a 50% increase in the area of land vulnerable to inundation is accompanied by a doubling of the number of land parcels potentially affected by flood water and a near doubling of roadways affected. By 2100, sea level rise produces significant additional encroachment of water into the north of the township of Port Fairy, into residential areas to the southwest of the Moyne River and between the river and Port Fairy Bay. There is also significant additional inundation at the northeast end of Belfast Lough, including at Griffiths Street. At Warrnambool, the additional area that becomes vulnerable to inundation by 2100 is somewhat dependent on the magnitude of sea level rise that takes place. Kelly Swamp may become vulnerable to inundation under scenario 1 while scenario 3 would also see Lake Pertobe becoming vulnerable to inundation. By 2100, scenario 1 produces a four-fold increase in the area of land, the number of land parcels and the length of roadway vulnerable to inundation. The increase in the number of land parcels and length of roadway exposed is almost six-fold for scenario 4.

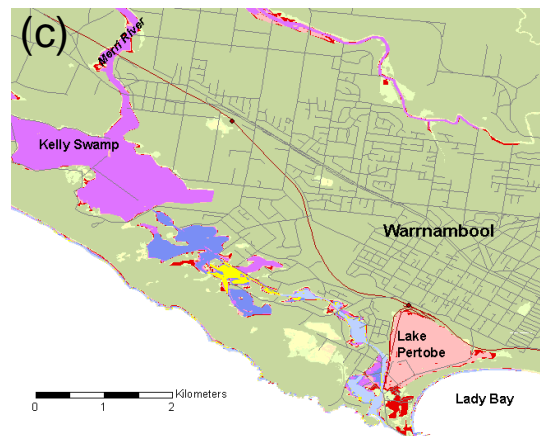
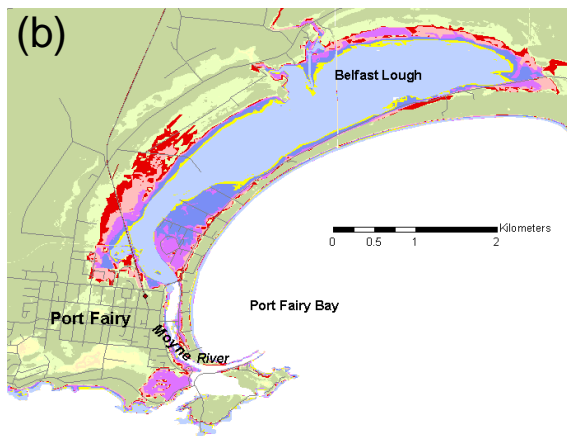
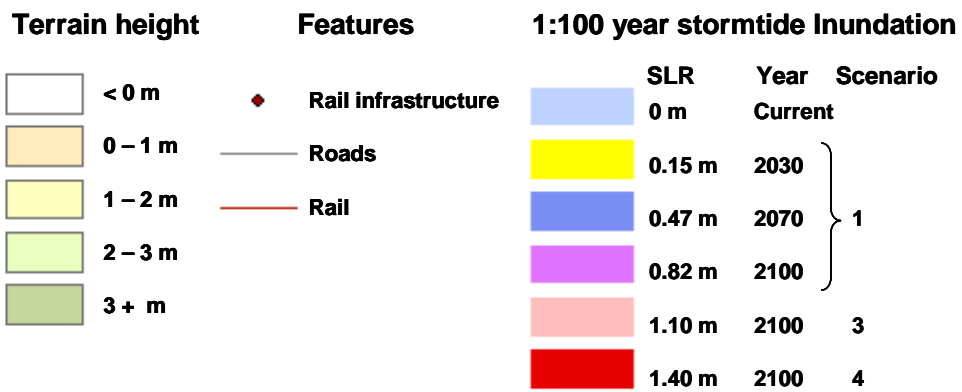
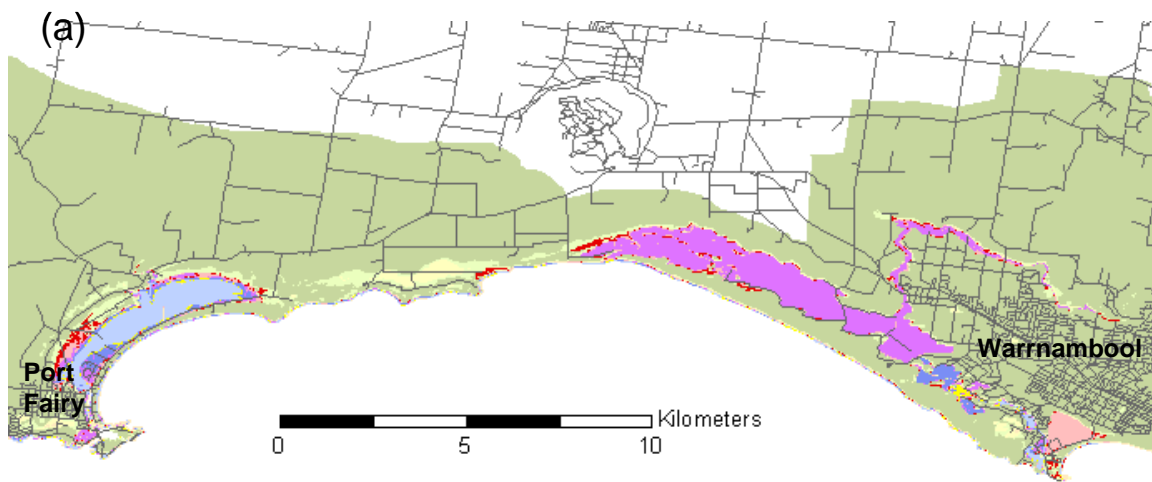


Figure 10: Land vulnerable to inundation during a 1 in 100 year storm tide under current climate conditions and various scenarios of future sea level rise for (a) the coastline from Port Fairy to Warrnambool, (b) Port Fairy and (c) Warrnambool

Table 8: Summary of the exposure of land parcels and roadways in the Port Fairy region to inundation under current climate conditions and various climate change scenarios.

Year	Scenario	Sea level rise m	Wind speed change %	Area of inundation km ²	Exposed land parcels	Exposed roadways km
Current climate		0	-	3.3	162	8.1
2030	1	0.15	-	3.7	168	10.7
	2	0.15	4	4.2	189	12.0
2070	1	0.47	-	5.0	314	14.3
	2	0.47	13	11.3	565	28.5
2100	1	0.82	-	12.4	680	32.9
	2	0.82	19	14.2	781	39.0
	3	1.10	-	14.0	812	39.5
	4	1.40	-	15.5	968	46.6

5.3 Barwon Heads

The Barwon Heads analysis region extends from the eastern edge of Torquay in the west to the western edge of Ocean Grove in the east. It contains extensive low-lying land associated with the Lower Barwon River estuary, Lake Conneware and Reedy Lake and low-lying swampland along the Thompson Creek at Breamlea (Figure 11).

Under current climate 1 in 100 year storm tide conditions, the lower reaches of the Barwon River, including Lake Conneware, Lake Conneware State Game Reserve and Reedy Lake, become inundated. The low-lying land adjacent to Thomson Creek behind the dune system at Breamlea and Point Impossible is also inundated as far eastwards as Breamlea Road. By 2030, sea level rise has a small additional effect on inundation along the Barwon River near Geelong and along Thomson Creek, scenario 1 adding less than 2 km² to the total area vulnerable to inundation. Under scenario 1, additional sea level rise by 2070 results in a 10% increase in the area of land vulnerable to inundation relative to the area for current climate conditions. Much of the additional vulnerable land is to the east of Breamlea Road, which is breached by the 1 in 100 year sea levels for 2070 associated with this scenario. However, additional inundation along the Barwon River in Ocean Grove results in a doubling of the number of land parcels vulnerable to inundation relative to the number for current climate conditions.

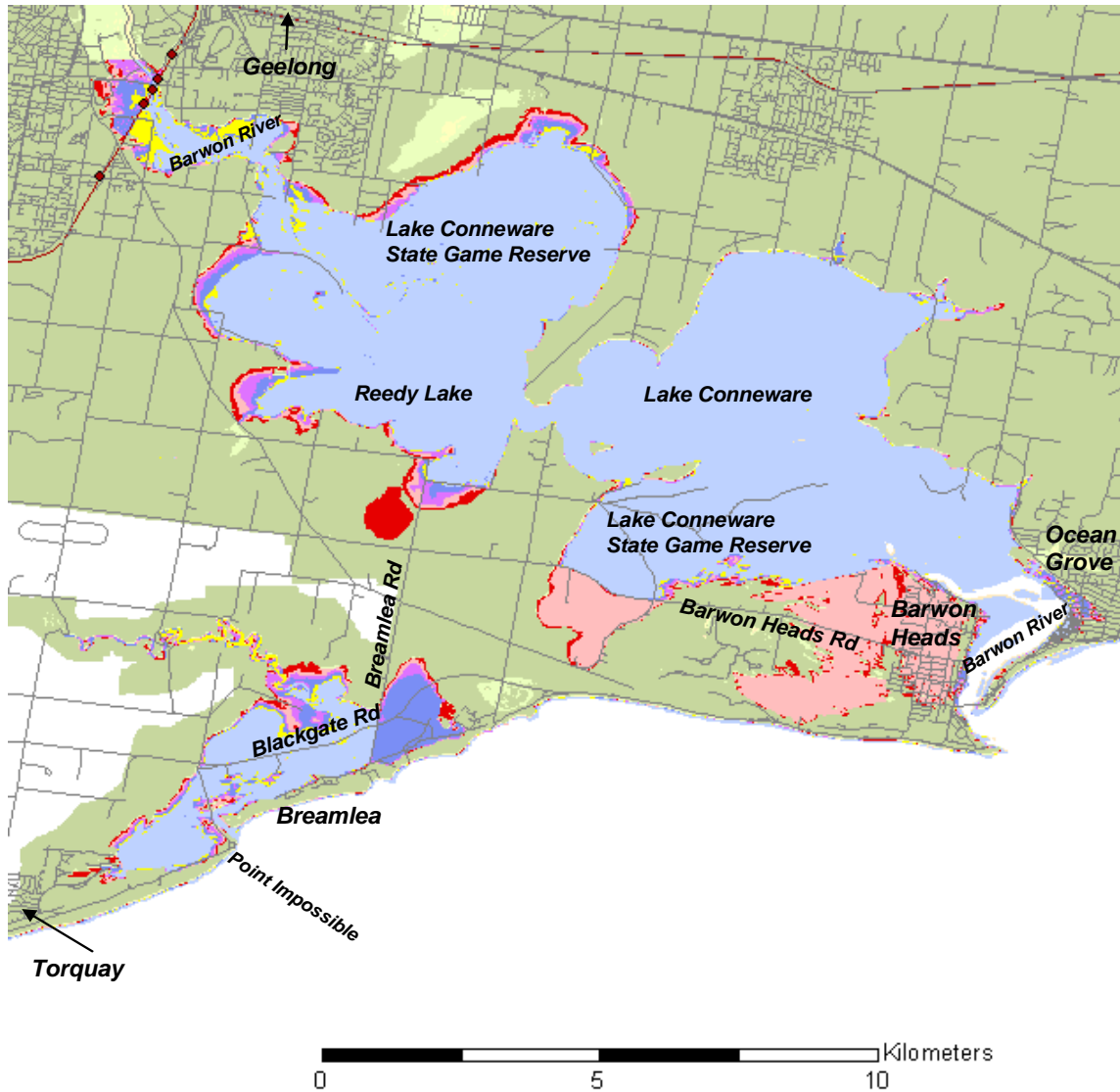


Figure 11: Land vulnerable to inundation during a 1 in 100 year storm tide under current climate conditions and various scenarios of future sea level rise for the Barwon Heads region.

The increase in the area of land vulnerable to inundation by 2100 is somewhat dependent on the magnitude of sea level rise that takes place. Under scenario 1, the area of land vulnerable to inundation does not increase greatly between 2070 and 2100. However, under scenarios 3 and 4, sea level rise results in a 30% increase in the area of land vulnerable to inundation relative to the area for current climate conditions, with in excess of 2500 properties in Barwon Heads becoming vulnerable to inundation. Large tracts of land to the north and south of Barwon Heads Road to the west of the township also become vulnerable to inundation.

Table 9: Summary of the exposure of land parcels and roadways in the Barwon Heads region to inundation under current climate conditions and various climate change scenarios.

Year	Scenario	Sea level rise m	Wind speed change %	Area of inundation km ²	Exposed land parcels	Exposed roadways km
Current climate		0	-	54.2	345	41.5
2030	1	0.15	-	56.0	460	52.9
	2	0.15	4	56.5	498	54.0
2070	1	0.47	-	59.6	693	65.6
	2	0.47	13	60.8	751	71.8
2100	1	0.82	-	61.9	821	76.2
	2	0.82	19	69.9	2559	106.7
	3	1.10	-	69.5	2591	108.6
	4	1.40	-	72.8	2825	116.3

5.4 Tooradin

The Tooradin analysis region is located on the northern shoreline of Western Port Bay. It contains mangrove-fringed marshland that will become increasingly prone to inundation under future sea level rise (Port of Melbourne, 1992). The extensive wetland and intertidal areas along the coast provide important habitats for bird and marine species. The main settlements in this region are Warneet and Tooradin.

Under current climate 1 in 100 year storm tide conditions, an extensive area of coastal land is potentially inundatable, with inundation also penetrating inland of the South Gippsland Highway between Cardinia Creek and Sawtells Inlet (Figure 12). Inland areas to the north of Warneet are also vulnerable with flooding occurring along the banks of Rutherford Inlet. Table 10 indicates that a total of 43 km² of land is vulnerable to inundation, although this is likely to be an overestimate because the inundation model does not take dynamic processes or the duration of storm surge events into account. By 2030 and 2070, the impact of sea level rise under scenario 1 increases the area vulnerable to inundation by approximately 15% and 50% respectively and increases the number of vulnerable land parcels by approximately 30% and 110% respectively. Much of the additional vulnerable land is to the north of the South Gippsland Highway. By 2100, more land in this area becomes vulnerable to inundation but significant areas of land in the western half of the analysis region also become vulnerable. The

total area that is vulnerable to inundation is 82 km², approximately double the area for current climate conditions, under scenario 1 and 110 km² under scenario 4. The increase in the number of land parcels exposed relative to the number for the current climate is approximately 160% under scenario 1 and approximately 200% under scenario 4.

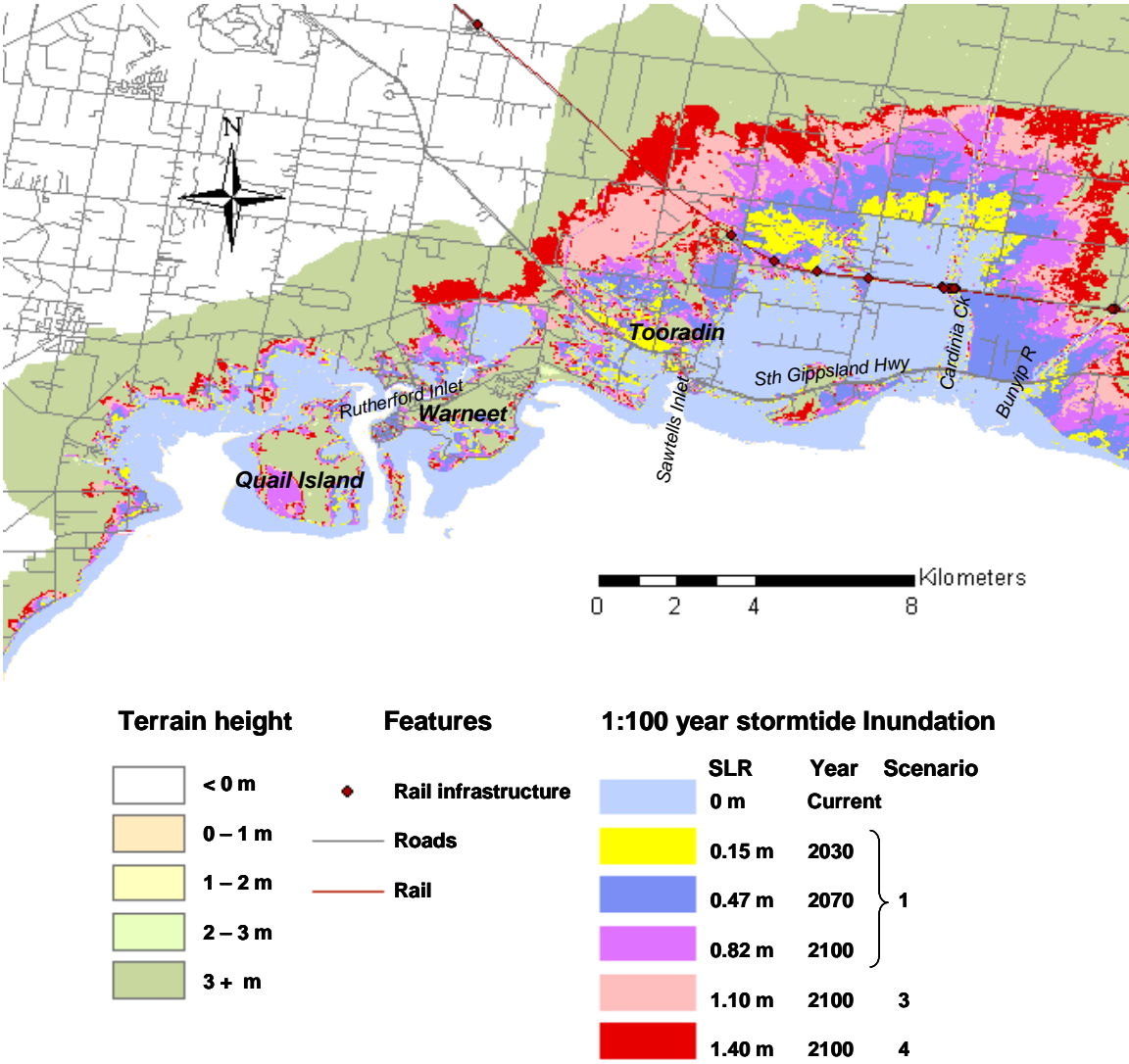


Figure 12: Land vulnerable to inundation during a 1 in 100 year storm tide under current climate conditions and various scenarios of future sea level rise for the Tooradin region

Table 10: Summary of the exposure of land parcels and roadways in the Tooradin region to inundation under current climate conditions and various climate change scenarios.

Year	Scenario	Sea level rise m	Wind speed change %	Area of inundation km ²	Exposed land parcels	Exposed roadways km
Current climate		0	-	42.6	554	61.7
2030	1	0.15	-	49.1	711	83.1
	2	0.15	4	52.5	822	94.3
2070	1	0.47	-	65.4	1161	124.8
	2	0.47	13	76.2	1343	141.8
2100	1	0.82	-	81.7	1425	151.9
	2	0.82	19	96.4	1587	173.5
	3	1.10	-	97.5	1574	172.0
	4	1.40	-	109.8	1704	192.7

5.5 Seaspray and The Honeysuckles

The fifth analysis region covers Seaspray and The Honeysuckles, two townships located behind Ninety Mile Beach in eastern Victoria. Ninety Mile Beach is backed by dunes that undergo considerable ‘cut and fill’ in response to wave action along the coast (Port of Melbourne, 1992). Behind the dunes are extensive backshore depressions and swamps, such as Lake Reeve to the northeast of the Merriman Creek and Lake Denison to the southwest (Figure 13).

Under current climate 1 in 100 year storm tide conditions, low-lying swamp areas associated with Lakes Reeve and Denison are vulnerable to inundation, as are the banks of the Merriman Creek. By 2030, the impact of sea level rise under scenario 1 results in a small additional increase in land area, of 3 km², that would be potentially affected by inundation. However, about half of this land area is located in the township of Seaspray and so the number of land parcels affected almost doubles. By 2070, the impact of sea level rise under scenario 1 results in a 30% increase in the area affected by inundation relative to the area affected under current climate conditions. The increase in exposed land parcels is more than six-fold, largely due to additional inundation in Seaspray. The Honeysuckles, which is located on higher ground than Seaspray, is not as impacted. However, the roadway connecting it to Seaspray is affected by inundation. By 2100, Seaspray, and significant sections of the roadway leading into the township, are completely inundated under any of the scenarios considered. Scenarios 3 and 4 also produce extensive inundation of The Honeysuckles. Under scenario 1, almost 3000 land parcels are affected by inundation and the length of roadway affected by is six times greater than for current climate conditions. Under scenario 4, approximately 3800 land parcels are affected by inundation and the length of roadway affected by is approximately seven times greater than for current climate conditions.

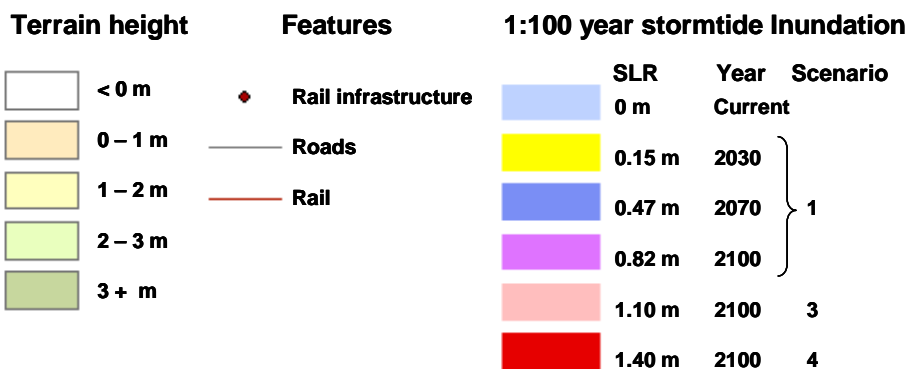
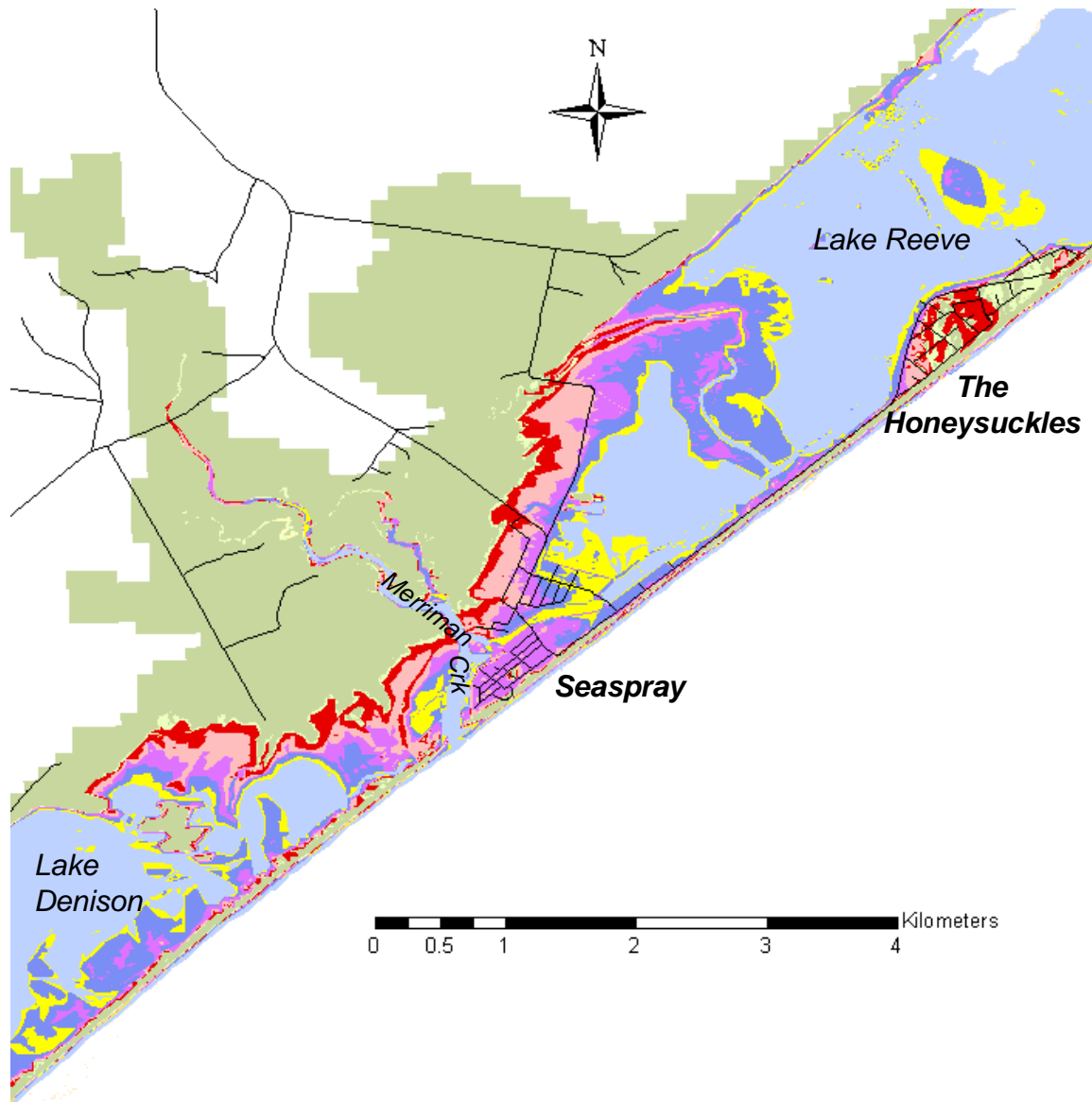


Figure 13: Land vulnerable to inundation during a 1 in 100 year storm tide under current climate conditions and various scenarios of future sea level rise for Seaspray and The Honeysuckles.

Table 11: Summary of the exposure of land parcels and roadways in the Seaspray region to inundation under current climate conditions and various climate change scenarios.

Year	Scenario	Sea level rise m	Wind speed change %	Area of inundation km ²	Exposed land parcels	Exposed roadways km
Current climate		0	-	27.4	289	8.4
2030	1	0.15	-	30.5	548	13.4
	2	0.15	4	31.3	579	14.1
2070	1	0.47	-	36.8	1867	30.5
	2	0.47	13	39.6	2720	44.1
2100	1	0.82	-	40.7	2984	50.0
	2	0.82	19	42.6	3341	52.9
	3	1.10	-	42.6	3346	52.9
	4	1.40	-	44.1	3763	58.0

6. SUMMARY AND FUTURE WORK

6.1 Summary and Discussion

This study builds upon earlier studies of the effect of climate change on extreme sea levels along the eastern Victorian coastline (McInnes et al., 2005a, b, 2006, 2007). It employs hydrodynamic modelling and statistical analysis to develop estimates of late 20th Century storm tide return levels along the entire Victorian coast and then explores the impact of a range of plausible climate change scenarios on these return levels. A DEM is used in combination with the estimated 1 in 100 year storm tide levels to identify land that may become vulnerable to inundation under the climate change scenarios considered.

This study finds that 1 in 100 year storm tide levels along the Victorian coast are highest in and around Western Port Bay, where they exceed 2.0 m under current climate conditions. Storm tide return levels are also high along the open coastline from just west of Port Phillip Heads to Wilsons Promontory, exceeding 1.8 m under current climate conditions. It should be noted that the methodology developed in this study, as well as the resolution of the hydrodynamic models and bathymetric and atmospheric data sets used, have been guided by the desire to provide data for the entire Victorian coast within the limitations of the available computing resources. It is possible that higher resolution studies of sections of the coastline utilising different methodologies and data sets may yield different return levels.

Four climate change scenarios were used to estimate storm tide return levels under future climate conditions and hence to investigate the impact of future climate change on coastal inundation. Hunter (2009) scaled the IPCC (2007) sea level rise figures for the end of the 21st Century to earlier decades throughout the century. The value derived from the IPCC's high-end sea level rise estimates for the SRES A1FI emissions scenario are consistent with recent observed trends in global carbon dioxide emissions and global mean sea levels and the Victorian Coastal Strategy (2008). These estimates, and higher estimates of sea level rise from the Netherlands Delta Committee and Rahmstorf (2007), formed the basis of three climate change scenarios that incorporated sea level rise only. A fourth scenario incorporated the high-end A1FI sea level rise estimates and high (90th percentile) estimates for changes in annual average wind speed for the A1FI emissions scenario obtained from recent climate change projections developed for Australia (CSIRO and Australian Bureau of Meteorology, 2007). However, it should be noted that, because of the large uncertainties in wind speed changes in Bass Strait represented by these projections, the possibility of future decreases in wind speed cannot be ruled out.

For the high-end A1FI sea level rise estimates considered, the contribution of consistent high-end estimates of wind speed increase to increases in extreme storm surge heights is considerably smaller, by a factor of more than two, than the contribution of sea level rise. It therefore seems likely that climate change will have a greater impact on extreme storm surge heights through sea level rise than through wind speed changes. It follows that sea levels currently attained only during severe storms will be reached during much less extreme conditions in the future. For example, at Portland, a storm tide of 1.01 m, the current 100-year

return level, may become a 1 in 20 year event by 2030, a 1 in 2 year event by 2070 and a sub-annual event by 2100. Indeed, if the Netherlands Delta Committee or Rahmstorf (2007) sea level rise estimates eventuate, and sea level rise exceeds 1.1 m, then low-lying parts of the coastline around Portland that are currently vulnerable to inundation by a 1 in 100 year storm tide will lie below the new mean sea level.

The potential inundation caused by a 1 in 100 year storm tide under various climate change scenarios was investigated. Five regions along the Victorian coast were selected for inundation analysis on the basis that they contained extensive areas of terrain below 2 m elevation. The main findings of the inundation analysis were that, under a 1 in 100 year storm tide, the most vulnerable areas were generally beach fronts, low-lying wetlands and coastal reserves.

Until after 2070, only small areas of the Portland region are vulnerable to inundation. By 2100, foreshore regions around Portland Harbour and Nuns Beach and the lower reaches of the Surry River, to the northeast of Portland, including low-lying terrain extending to the east and west of the river, become vulnerable to inundation under 1 in 100 year storm tide conditions.

In the Port Fairy region, the banks of the Moyne River and Belfast Lough at Port Fairy and the lower reaches of the Merri River at Warnambool are vulnerable to inundation under current climate 1 in 100 year storm tide conditions. The effect of climate change on inundation is minimal until after 2030. However, by 2070, extensive additional areas adjacent to Belfast Lough at Port Fairy and the Merri River at Warnambool may become vulnerable to inundation. By 2100, additional areas at the northeast of Belfast Lough, in Port Fairy township and Kelly Swamp, and, if sea level rise exceeds that of scenario 3, Lake Pertobe, at Warnambool may become vulnerable to inundation.

In the Barwon Heads region, the lower reaches of the Barwon River and low-lying land behind the dune system at Breamlea are vulnerable to inundation under current climate 1 in 100 year storm tide conditions. By 2030, a small additional area along the Barwon River near Geelong and along Thomson Creek may become vulnerable. By 2070, parts of Ocean Grove adjacent the Barwon River and low-lying land east of Breamlea may become vulnerable. By 2100, if sea level rise exceeds that of scenario 3, extensive inundation to the west of Barwon Heads and complete inundation of the township may occur under 1 in 100 year storm tide conditions.

In the Tooradin region, an extensive area of coastal land, areas inland of the South Gippsland Highway between Cardinia Creek and Sawtells Inlet and inland areas to the north of Warneet are vulnerable to inundation under current 1 in 100 year storm tide conditions. Incrementally more extensive areas north of the South Gippsland Highway may become vulnerable as the 21st Century progresses. By 2100, significant additional areas west of Tooradin may also become vulnerable to inundation under 1 in 100 year storm tide conditions.

In the Seaspray region, Lakes Reeve and Denison and the banks of the Merriman Creek are vulnerable to inundation under current 1 in 100 year storm tide conditions. By 2030 and 2070, incrementally larger parts of the township of Seaspray may become vulnerable. By 2100, complete inundation of the township of Seaspray and, if sea level rise exceeds that of scenario 3, extensive inundation of the The Honeysuckles may occur under 1 in 100 year storm tide conditions.

6.2 Recommendations for Future Work

In this study, extreme sea levels due to the combination of storm surges and tides have been estimated. As indicated in Figure 1, waves can also contribute to extreme sea levels through wave setup and wave runup. Estimating the contribution of waves to extreme sea levels, which is generally much smaller than that of a storm surge, was beyond the scope of the present study. However, a preliminary study of wave setup during storm surge events has shown that coastline orientation in relation to the prevailing winds and waves during a storm event will strongly determine the magnitude of wave setup at the coast (McInnes et al. 2009b). Future work should aim to quantify the contribution of waves to sea level extremes along the Victorian coastline. High resolution bathymetric Lidar data sets that are being developed as part of the Future Coasts Program will be important to this endeavour.

The inundation analysis presented in this report was performed using a simple technique that does not take into account some of the physical factors that will influence the degree of inundation that will occur. Notably, there is no accounting for how flood water currents are impeded by friction at the terrain surface or the dependence of inundation on the duration of the storm tide. These effects would be expected to limit the inland penetration of water during a temporary elevation of coastal sea levels and their omission in this study may have led to an overestimation of the degree of inundation. However, it should be noted that these limitations apply only to the storm tide component of extreme sea levels and not the mean sea level rise component. Sea level rise results in a sustained contribution to total sea level, which can lead to permanent inundation of low-lying coastal land. Future work may seek to quantify any overestimation of inundation by explicitly modelling the temporal evolution of inundation during a storm tide event. Inundation simulations could be performed using a high resolution hydrodynamic model with a wetting and drying algorithm.

The storms associated with storm tides are often accompanied by significant rainfall in river catchments intersecting the coastal zone. Hence, in addition to coastal inundation due to extreme sea levels, a storm tide may also be accompanied by inundation due to rainfall. This additional contribution to inundation, which is not taken into account in this study, would potentially increase the area affected by inundation. Investigation of the potential for coincident storm tide and heavy rainfall events in the Victorian region under current and future climate conditions would therefore be of benefit.

This study has regarded the topography of the coastline as being constant throughout the 21st Century. However, during this time period, environmental processes, such as the erosion of beaches and soft cliffs, have the potential to change the morphology of the shoreline. Indeed, many of these processes will be affected by increases in mean and extreme sea levels associated with climate change and hence climate change itself may result in significant changes in the shoreline in the future. Superimposed on these environmental processes will be the adaptive responses of society to changes in the shoreline. Such adaptive responses may include the continuing renourishment of beaches to retain the existing coastline, the building of sea walls along the coast and embankments along water courses to inhibit erosion and inundation and the infilling of low-lying land. The consideration of environmental processes that change the shoreline and adaptive responses should be priority areas of future work.

Despite various limitations, the analysis presented in this study illustrates how different climate change scenarios may affect the degree of inundation that could potentially occur due to extreme sea levels in the future. The study identifies areas that will be most vulnerable to coastal inundation in the future and highlights thresholds of sea level rise that are important in the context of vulnerability and adaptation.

ACKNOWLEDGMENTS

Tide gauge data were provided by the National Tidal Centre, Port of Melbourne Corporation and Melbourne Water. The authors are grateful to Drs. Ben Preston, Graeme Hubbert and Catia Domingues for advice on aspects of the work undertaken in this study. Some of this work draws upon earlier work that was funded by the Australian Greenhouse Office and the Antarctic Climate and Ecosystem CRC.

REFERENCES

Australian National Tide Tables, 2007: Australian Hydrographic Service. ISSN 0812-2245. 404pp.

Church, J.A., and White, N.J., 2006: A 20th Century acceleration in global sea-level rise. *Geophys. Res. Lett.*, doi:10.1029/2005GL024826.

Coles, S.G., 2001: *An Introduction to Statistical Modeling of Extreme Values*. Springer.

CSIRO and Australian Bureau of Meteorology, 2007: *Climate Change in Australia*, CSIRO and Bureau of Meteorology Technical Report, 140 pp. www.climatechangeinaustralia.gov.au.

Foreman, G.G., 1997: *Manual for Tidal Heights Analysis and Prediction*, Pacific Marine Science Report 77-10, Institute of Ocean Sciences, Victoria, Canada, 98pp.

Godin, G., 1972: *The Analysis of Tides*. University of Toronto Press.

Gurran, N., Squires, C., and Blakely, E., 2005: Planning for Sea Change in Coastal Australia, *Australian Planner*, 42(4), 10-11.

Hubbert, G.D., 1993a: Modelling continental shelf flows along the New South Wales coast with a fully three dimensional ocean model. Proc. 11th Australasian Coastal and Ocean Engineering Conference, Townsville, Australia.

Hubbert, G.D., 1993b: Oil spill trajectory modelling with a fully three dimensional ocean model. Proc. 11th Australasian Coastal and Ocean Engineering Conference, Townsville, Australia.

Hubbert, G.D., and McInnes, K.L., 1999: A storm surge inundation model for coastal planning and impact studies., *J. Coastal Research*, 15, 168-185.

Hunter, J., 2009: Estimating Sea-Level Extremes Under Conditions of Uncertain Sea-Level Rise. *Climatic Change*. DOI 10.1007/s10584-009-9671-6.

IPCC, 2007: Contribution of Working Group I to the Fourth Assessment Report of the Intergovernmental Panel on Climate Change. Summary for Policymakers. 18pp <http://www.ipcc.ch/SPM2feb07.pdf>

IPCC, 2000: Special Report on Emission Scenarios: A Special Report of Working Group III of the Intergovernmental Panel on Climate Change. Cambridge University Press.

IPCC, 2001: *Climate Change 2001: The Science of Climate Change*. Summary for Policymakers and Technical Summary of the Working Group I Report. Intergovernmental Panel on Climate Change. Cambridge University Press, v+ 98 pp.

Kalnay, E., Kanamitsu, M., Kistler, R., Collins, W., Deaven, D., Gandin, L., Iredell, M., Saha, S., White, G., Woollen, J., Zhu, Y., Leetmaa, A., Reynolds, B., Chelliah, M., Ebisuzaki, W.,

Higgins, W., Janowiak, J., Mo, K.C., Ropelewski, C., Wang, J., Jenne, R., and Joseph, D., 1996: The NCEP/NCAR 40-Year Reanalysis Project. *Bull. Amer. Meteor. Soc.*, 77, 437–471.

Le Provost, C., Bennett, A.F., and Cartwright, D.E., 1995: Ocean tides for and from TOPEX/POSEIDON. *Science* 267: 639-642.

McInnes, K.L., and Hubbert, G.D., 2003: A numerical modeling study of storm surges in Bass Strait. *Aust. Met. Mag.* 52, 143-156.

McInnes, K.L., Abbs, D.J., and Bathols, J.A., 2005a: Climate Change in Eastern Victoria Stage 1 Report: The effect of climate change on coastal wind and weather patterns. CSIRO Consultancy Report for the Gippsland Coastal Board. 26pp.

McInnes, K.L., Macadam, I., Hubbert, G.D., Abbs, D.J., and Bathols, J.A., 2005b: Climate Change in Eastern Victoria Stage 2 Report: The effect of climate change on storm surges. CSIRO Consultancy Report for the Gippsland Coastal Board. 37pp.

McInnes, K.L., Macadam, I., and Hubbert, G.D., 2006: Climate Change in Eastern Victoria. Stage 3 Report: The effect of climate change on extreme sea levels in Corner Inlet and the Gippsland Lakes. Report to Gippsland Coastal Board. July 2006, 40 pp.
http://www.cmar.csiro.au/e-print/open/mcinnesk_2006a.pdf

McInnes, K.L., Macadam, I., and O’Grady, J.G., 2007: The Effect of Climate Change on Extreme Sea Levels in the Westernport Region A Project Undertaken for the Australian Greenhouse Office and Department of Sustainability and Environment, Victoria, 24pp.

McInnes, K.L., Macadam, I., Hubbert, G.D., and O’Grady, J.G., 2009a: A Modelling Approach for Estimating the Frequency of Sea Level Extremes and the Impact of Climate Change in Southeast Australia. *Natural Hazards* DOI 10.1007/s11069-009-9383-2.

McInnes, K.L., O’Grady, J.G., and Hubbert, G.D., 2009b: Modelling sea level extremes from storm surges and wave setup for climate change assessments in southeastern Australia. *J. Coastal Res.* SI56 1005-1009.

McInnes, K.L., O’Grady, J.G., and Macadam, I., 2009c: The effect of climate change on extreme sea levels in Port Phillip Bay. Report to Victorian Department of Sustainability and Environment. 56pp.

Nakićenović, N., and Swart, R., (eds.), 2000: Special Report on Emissions Scenarios. A Special Report of Working Group III of the Intergovernmental Panel on Climate Change, Cambridge University Press, Cambridge, United Kingdom and New York, NY, USA, 599pp.

Port of Melbourne Authority (1992), Victorian Coastal Vulnerability Study. Coastal Investigations Unit, Port of Melbourne Authority, Port Melbourne, VIC. 60pp.

Pugh, D.T., and Vassie, J.M., 1980: Applications of the joint probability method for extreme sea level computations. *Proc. Instn. Civ. Engrs.* 69, 959-975.

Rahmstorf, S., 2007: A semi-empirical approach to projecting future sea-level rise. *Science*, 315(5810), 368–370.

Raupach, M.R., Marland, G., Ciais, P., Le Quéré, C., Canadell, J.G., Klepper, G., and Field, C.B., 2007: Global and regional drivers of accelerating CO₂ emissions. *Proceedings of the National Academy of Sciences of the USA*, 104, 10288–10293.

Tawn, J.A, and Vassie, J.M., 1990: Spatial transfer of extreme sea level data for use in the revised joint probability method. *Proc Inst Civil Eng Part 2* 89:433–438

Vellinga, P., 2008: Exploring high end climate change scenarios for flood protection of the Netherlands. *International Scientific Assessment*, 136pp.

Watterson, I.G. 2008: Calculation of probability density functions for temperature and precipitation change under global warming. *J. Geophys. Res.*, 113, D12106, doi:10.1029/2007JD009254.



Contact Us

Phone: 1300 363 400

+61 3 9545 2176

Email: enquiries@csiro.au

Web: www.csiro.au

Your CSIRO

Australia is founding its future on science and innovation. Its national science agency, CSIRO, is a powerhouse of ideas, technologies and skills for building prosperity, growth, health and sustainability. It serves governments, industries, business and communities across the nation.